AN EXPERIMENTAL STUDY OF THE DIPOLE ANTENNA WITH NONREFLECTING RESISTIVE LOADING

Scientific Report No. 7

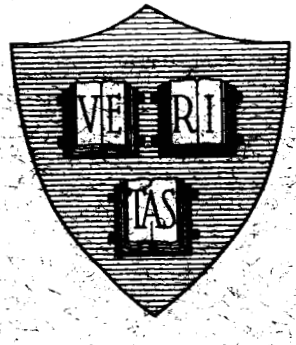

By

Liang-Chi-Shen

September 1966

NATIONAL AERONAUTICS AND SPACE ADMINISTRATION

Prepared under Grant No. NsG 579

Gordon McKay Laboratory, Harvard University
Cambridge, Massachusetts

AN EXPERIMENTAL STUDY OF THE DIPOLE ANTENNA WITH NONREFLECTING RESISTIVE LOADING

By

Liang-Chi Shen

Scientific Report No. 7

September, 1966

Prepared under Grant No. NsG 579 at
Gordon McKay Laboratory, Harvard University
Cambridge, Massachusetts

for

NATIONAL AERONAUTICS AND SPACE ADMINISTRATION

AN EXPERIMENTAL STUDY OF THE DIPOLE ANTENNA WITH NONREFLECTING RESISTIVE LOADING

Liang-Chi Shen

Gordon McKay Laboratory, Harvard University
Cambridge, Massachusetts

ABSTRACT

The amplitude of the current, the input admittance, and the radiation field pattern of a cylindrical antenna with a step-function internal impedance are measured in the frequency range 450 to 900 MHz. Several designs of the step-function are tried in order to simulate the antenna with the smoothly distributed resistive loading which has been studied in previous reports. The experimental result is compared with the theory. It is pointed out that such comparison is meaningful in the light of the analysis carried out in previous reports. It has been found that the zero-order theory gives accurate descriptions of the current distribution, the field pattern, the property of a very broad frequency band of the antenna, and the existence of the traveling wave on the antenna. The agreement of the input admittance is not good, but it is found that the theoretical input admittance of the infinitely long resistive antenna which is obtained by a Fourier Transform method fits the experimental data satisfactorily.

1. Introduction

Traveling wave antennas are desirable for purposes of broadband and directional communication. A traveling wave antenna may be obtained by introducing dissipative elements into the antenna system [1], [2]. The introduction of lossy element will inevitably result in a decrease in efficiency, but the loss of overall efficiency in a transmitting system is often the price to be paid for an improvement in the broadband and the directional properties. If the lossy element is not added in the antenna itself, it may be added to the feeding network in order to make the system broadband however, the traveling-wave property is then not achieved. On the other hand, efficiency should not be of major concern in a receiving antenna for which the requirements of a broadband, directivity and a simplicity of structure are usually the most important factors. Resistive antennas are being designed for use in satellite communication.

In Altshuler's work [1] it is found that a traveling wave may exist on an antenna with lumped resistors located a quarter wavelength from the ends of the antenna. However, since the location of the resistor depends linearly on the wavelength, such an antenna cannot have a very broad band. Furthermore, the resistance of the resistor cannot be known beforehand. In fact, resistors with d-c resistance ranging from 3 ohms to 1 megohm had to be tested separately on the antenna in Altshuler's experiment in order to find the suitable resistor which could induce a traveling wave on it.

In the work of Wu and King [2] it is found that if the antenna is made of resistive material such that z^i, the internal impedance per unit length, is

a particular function of the position along the antenna, a pure outward traveling wave can exist on an antenna of finite length. It is found that if

$$z^i(z) = \frac{\zeta_o \Psi}{2\pi} \frac{a}{h - |z|} \tag{1}$$

then the zero-order current is

$$I(z) = \frac{2\pi}{\zeta_o \Psi (1+i/kh)} (1 - |z|/h)\, e^{ik|z|} \quad \text{for } a = 1 \tag{2}$$

The constant Ψ is determined by

$$\Psi\, |I(z)| = \left| \int_{-h}^{h} I(z')\, e^{ikR}/R \; dz' \right| \tag{3}$$

at the maximum of $I(z)$, where $R = [(z-z')^2 + a^2]^{\frac{1}{2}}$. In the above equations, z is the axial coordinate, ζ_o is the intrinsic impedance of free space, h is the half-length of the antenna, k is the free-space wave number, and a is the radius of the antenna. The antenna is assumed to be driven by a delta-function generator which has time dependence $e^{-i\omega t}$ and an emf of one volt. Note that here the distribution of the z^i along the antenna that is necessary to support a traveling wave is determined predominantly by the physical distance rather than the electrical distance, with the frequency dependence appearing only in Ψ in the form of a logarithm [ref. 2, Eq. 29]. Therefore the antenna should have a very broad-band. Moreover, the current distribution (2) is a simple function which can be easily integrated to get the field pattern.

The purpose of this experiment is to measure the current distribution, the input admittance, and the radiation field pattern of the cylindrical antenna with nonreflecting resistive loading in order to compare them with the theory of Wu and King [2]. Due to technical reason , antennas with z^i varying in the form of steps rather than in continuously varying fashion have been built. Various designs of this step antenna have been tried in order to simulate the continuously loaded antenna.

From the analytic point of view, the antenna with step-function z^i is inconvenient. In an analysis carried out by Shen and Wu [3] the parameter a in (1) is not restricted to unity as it is in [2]. Hence the stepwise variation of z^i can be viewed as the discontinuity of the parameter a in (1) and it has been concluded in [3] that the effect of the perturbation of a on the current distribution and therefore the field pattern is small for a near 1. In this sense the comparison between the theory and the measured result of the antenna with step-function z^i becomes meaningful.

In this experiment the frequency range is chosen to be from 450 to 900 MHz. A higher frequency range would cause difficulty in the construction of, among other things, electrically small probes . In addition to this reason, the difficulty in obtaining the right material to make the effect resistive coating at higher frequencies is also a major factor. The indoor metallic image plane which was available for this experiment restricts the use of lower frequency range.

The internal impedance of the antenna to be measured here is many times higher than that of the ordinary brass antenna; such high resis-

tivity is obtained by spraying resistive paint on a dielectric cylindrical rod. In order to be able to measure the internal impedance after the rod has been sprayed, the thickness of the resistive coating must be made smaller than the skin depth of the resistive material at the frequency range mentioned earlier. Therefore the d-c resistance of the coated rod, which can be measured easily and accurately, would be a good indication of the internal impedance of the coating in the r-f field. Inasmuch as the coating is thin, the field due to the antenna penetrates into the coating and the ordinary internal probe with metallic coaxial transmission line cannot be used to measure the current distribution on the antenna. An external probe with a series of detuning sleeves built on the coaxial conductor in order to minimize the current excited on the lead wire [4] will not work either because in the present case the operating frequency is not fixed. An external probe with diode rectifier attached to the loop and with high resistive wires used as leads is thus proposed. A diode rectifier, however, can only detect the amplitude of the field, the other important information about the phase of the field is sacrificed. Thus in this experiment the antenna will be shown to have a relatively invariable distribution of the amplitude current, of the driving-point admittance, as well as, the field pattern against changing frequency, which we shall consider as a proof that the antenna has a broadband. The directional character of the antenna will be domonstrated by measuring the field pattern of the V-antenna which is formed by folding down the two arms of the dipole antenna.. The existence of a traveling wave on the antenna is not demonstrated directly but is believed that it will be suggested by the experimental results.

The physical length of the antenna that will be under test is chosen to be 50 cm long, or 1 wavelength long at 600 MHz. The reason for this choice is as follows. As a result of previous theoretical analysis, the radiation efficiency of the antenna is known to increase as the antenna becomes longer (see ref. 3 Fig. 10). For this reason a longer antenna length is favoured. With a longer antenna the difference between the theory and the experiment can be seen more clearly since the former is only of zero-order accuracy as radiated power has not been taken into account. However, the limited size of the indoor ground plane restricts the antenna length on one hand and on the other hand longer resistive wires are needed for a longer antenna in order to feed the signal detected by the diode from the loop to the measuring equipment, consequently the signal-to-noise ratio is reduced. Perhaps the dominant factor that limits to 50 cm is the fact that if the length is increased the required internal impedance near the driving point would become too low to be obtained in the laboratory.

2. <u>The Free-Space Room, The Transmitting System, and the Detecting System for Current and Admittance Measurements</u>

For the measurements of current distribution and driving-point admittance of the antenna, a metallic image plane is used, as usual, so that the observer and the equipment are completely out of the field due to the antenna under test. The ground plane used in this experiment is made of $\frac{1}{4}$-inch aluminum plates. It is 305 cm high, 366 cm wide and is surrounded by absorbing materials to form a room about 244 cm high, 330 cm wide, and 208 cm long. The antenna is located near the center of the ground plane.

The detail structure of this free-space room and the ground plane can be found in Whiteside's work [5], who originally designed it in 1962 for experimental study of various probes. While his concern was mainly over the near field of an antenna operating at 600 MHz, it is found that the room is also suitable for purpose of current distribution and input admittance measurements over the frequency range of 450 to 900 MHz. For purpose of testing the facility, the current distribution,and the input admittance of an ordinary brass monopole antenna have been measured by conventional shielded loop probe with superheterodyne detection over the frequency range just mentioned. The antenna was made of brass tubing with hemispherical cap at its end; the slot along the antenna was 0.159 cm wide. The slot was covered with a brass slab during the measurement of the input admittance. The antenna was supported by a polyfoam table with relative dielectric constant equal to 1.04 approximately. The results of the measurements are shown in Fig. 1 and 2 and they are found to be in good agreement with both the theory [6] and the experimental data obtained by others [7]. It is felt that this test gives a good indication of the usefulness of this free-space room for current and input admittance measurements in the frequency range of 450 to 900 MHz.

The transmitting system consists of an UHF oscillator made by the General Radio Company of Massachusetts (Type 1361-A) with modulating power supply (Type 1264-A) which can provide either CW or 1 KHz square wave modulation. The frequency range of the oscillator is from 450 to 1050 MHz and the frequency can be set within 0.2 percent of accuracy by means of a vernier scale dial once calibration has been done. The frequency

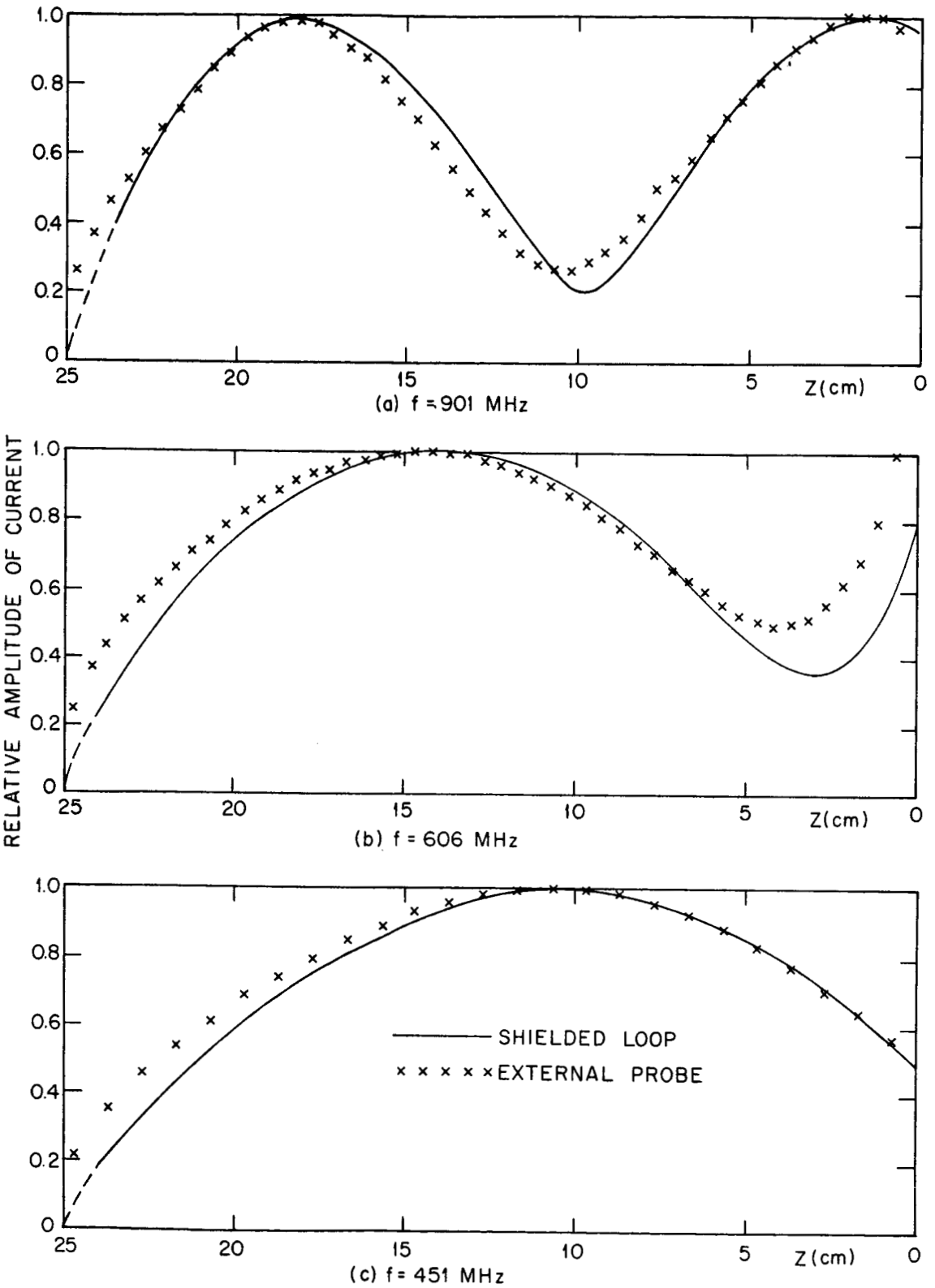

FIG. 1 THE CURRENT DISTRIBUTION ON A BRASS ANTENNA

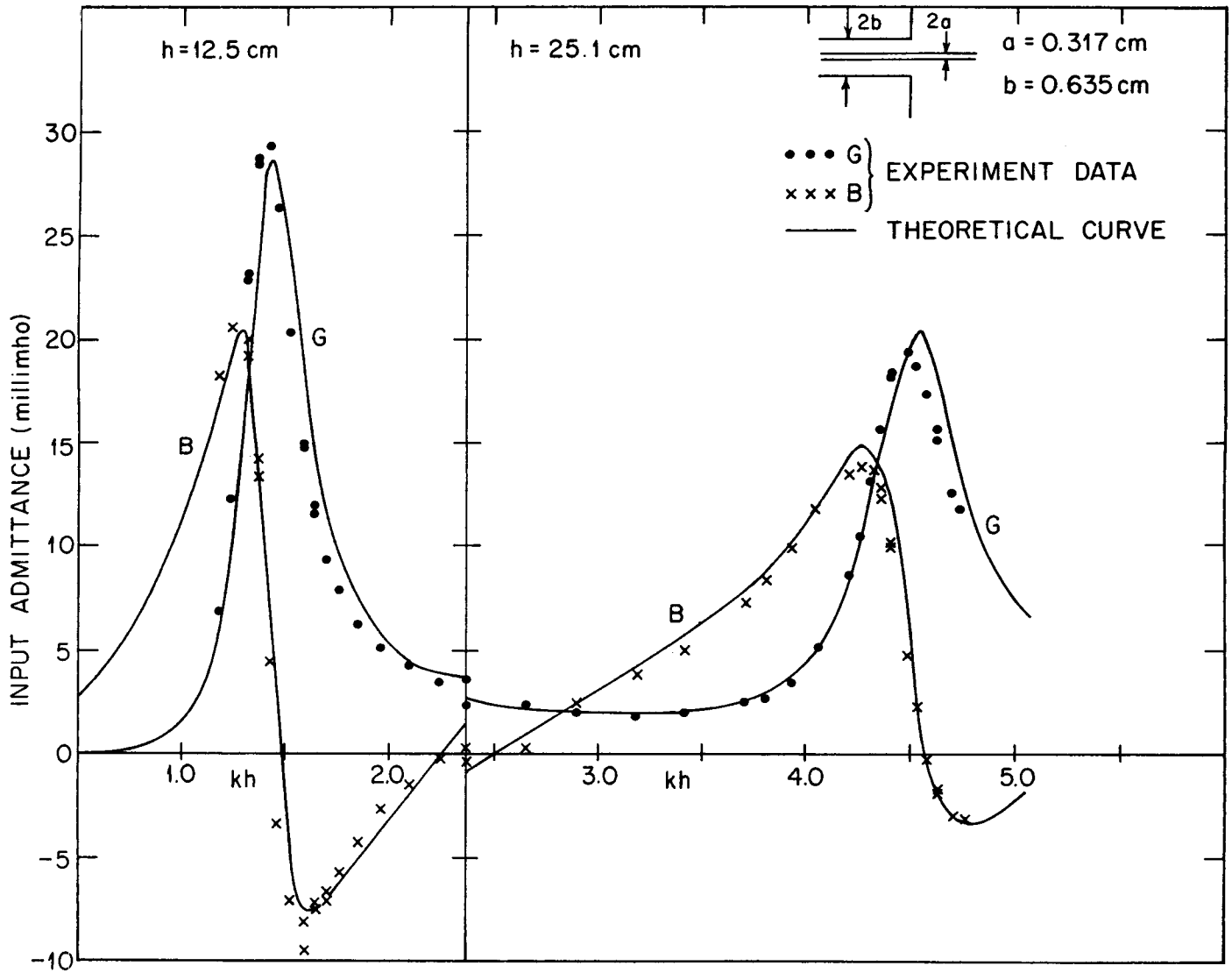

FIG. 2 INPUT ADMITTANCE OF MONOPOLE BRASS ANTENNA AT DIFFERENT FREQUENCIES

drift due to the loading of the oscillator is found to be no more than 0.2 percent.

The output of the oscillator is fed into a coaxial line at a T-junction. The inner diameter of the outer conductor of the coaxial line is 1.27 cm, and the outer diameter of the slotted inner conductor is made out of a brass tubing with 0.488 cm i.d.. The internal probe travels within this inner conductor. The distance from the T-junction of the coaxial line to the driving point where the antenna is connected 70 cm, of which 60 cm is continuously filled with polyfoam and the 10 cm near the junction is not filled. The relative dielectric constant of the polyfoam was measured to be 1.052. There is a movable piston behind the T-junction for the purpose of tuning.

If the internal probe is a shielded loop, as in the measurement of the input admittance and the current distribution on the brass antenna, superheterodyne detection is employed. It involves an UHF oscillator (Type 1209-B, frequency range from 250 to 920 MHz), with regulated power supply (Type 1201-B), a mixer (Type 874) and an I.F. amplifier (Type 1216-A), all made by General Radio Company.

For the detection of a signal picked up by the external probe with the diode rectifier, a high input impedance (40 K-ohms) voltage amplifier is used to boost the signal fed through the resistive leads. The output of the amplifier is connected to a band-pass filter to pass a 1 KHz audio signal. The signal is then fed into an oscilloscope where the amplitude is read. The highest reading on the oscilloscope is kept under 0.5 volt as a precaution against nonlinear amplification due to saturation of the amplifier. The oscilloscope was made by Tektronix Incorporated of Oregon (Type 532

with Type B plug in unit), it is capable of displaying a signal from 0.05 volt per cm to 0.005 volt per cm in 4 steps. The band pass filter was manufactured by the United Transformer Corporation of New York (Model 4c). The voltage amplifier was made by the Acoustic Laboratory of Harvard University. A block diagram showing the arrangement of the detecting system is illustrated in Fig. 3.

3. The External Probe

The external probe consists of a silicon video detector diode (model number MA-4123A manufactured by Microwave Associates of Massachusetts) and a capacitor of 330×10^{-12} farad d-c capacitance which, together with the diode, forms a square loop about 1 cm $\times$ 1 cm in dimensions. The diode is 0.24 cm in diameter and is 0.75 cm long, and the capacitor is of similar dimensions. Two strings of resistors, with resistors spaced about 3.0 cm from center to center, are connected to the two sides of the loop serving as two leads for the detected audio signal (see Fig. 4). The first section of the resistive wires is erected vertically, is perpendicular to the antenna under measurement, and is about 50 cm long. It consists of resistors with 390 ohms d-c resistance, 5% precision, and $\frac{1}{2}$ wattage rating, except the two resistors nearest to the loop which are 470 ohms with 10% precision and 1/8 wattage rating. The second section of the resistive wires is horizontal, is parallel to the antenna, and is about 55 cm long, while the d-c resistance of each resistor is 200 ohms with 5% precision and $\frac{1}{2}$ wattage rating. The total d-c resistance of each wire is about 10 K-ohms. Resistors are soldered together and the two resistive wires are confined in a plexiglass tube of 1.27 cm o.d. and 0.94 cm i.d.,

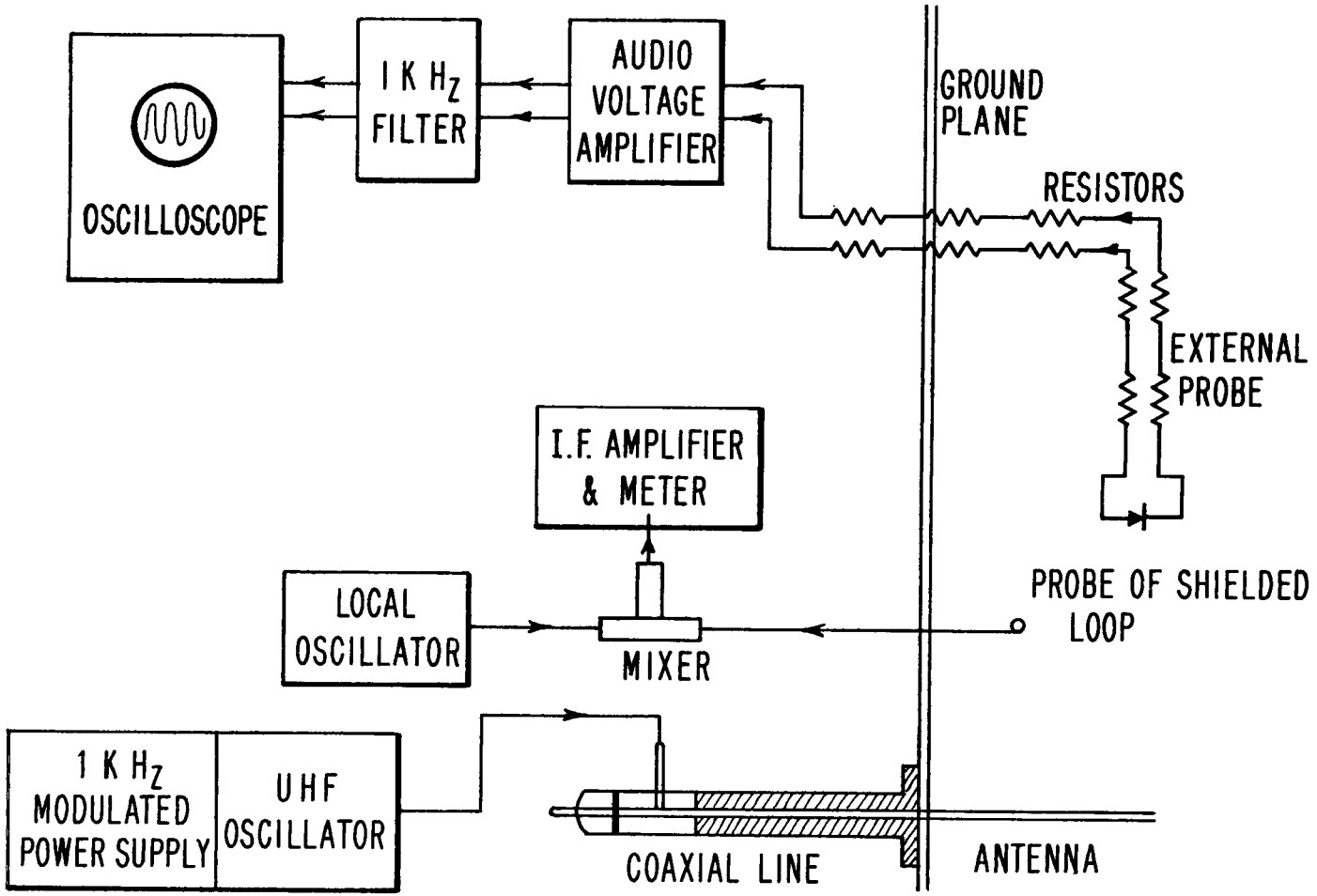

FIG. 3 BLOCK DIAGRAM OF THE TRANSMITTING AND THE DETECTING SYSTEM.

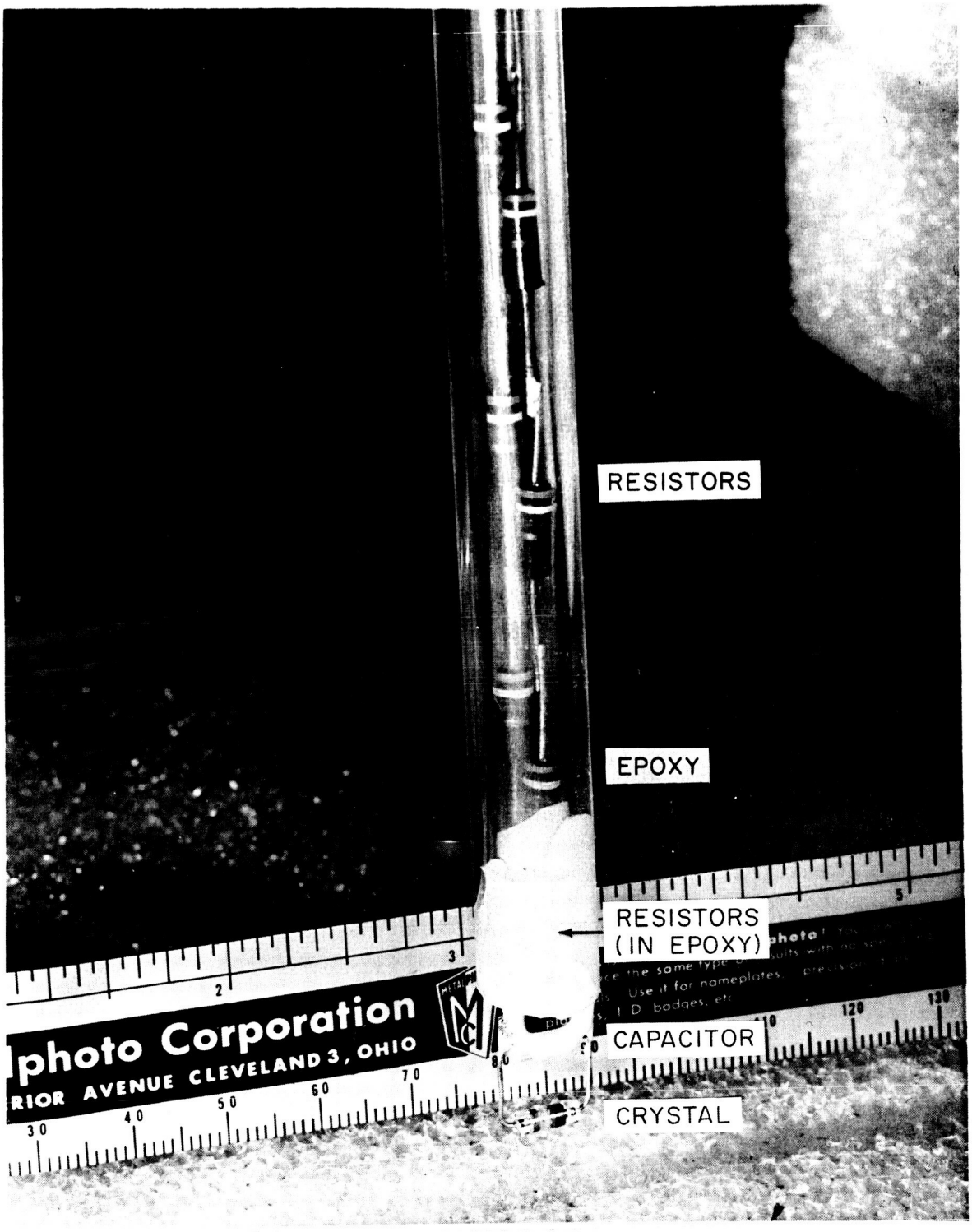

FIG. 4 THE EXTERNAL PROBE

and they are cemented by epoxy material at several places in order to secure the junction and prevent the wires from short-circuiting.

The vertical section of the resistive wires is further embedded in a polyfoam block which in turn rests on a polyfoam platform so that they form an inverted T-shaped structure (see Fig. 5). The horizontal section of the resistive wire is at one end connected to the vertical section of the wire at the top of the inverted-T and the other end of it goes through and rests freely in a hole on the ground plane and leads to the audio amplifier.

At the bottom of the polyfoam platform there are two teflon wheels on one side and a set of two keys on the other side. The wheels can roll or slide in a track which is embedded in a polyfoam table on which the whole structure rests, including the antenna under measurement. The keys are to lock the platform in position while it is being moved. The track is made of a slotted plexiglass tube of 0.70 cm o.d. and 0.32 cm i.d., so that the platform can hardly be shifted either sideways or upward as it is moved by a horizontal force along the direction of the antenna.

The polyfoam platform as well as the external probe can be moved at the back of the ground plane by means of a plexiglass rod of 1.02 cm in diameter. This rod is firmly attached to the platform at one end, goes through a hole on the ground plane and has an indicator attached at the other end. The indicator rests on a steel scale to register the position of the external probe. The rod is 19.2 cm away from the center of the antenna and is 10.0 cm above the polyfoam table.

As the polyfoam platform is pushed by means of the plexiglass rod and moves along the track, it is found that the distance between the

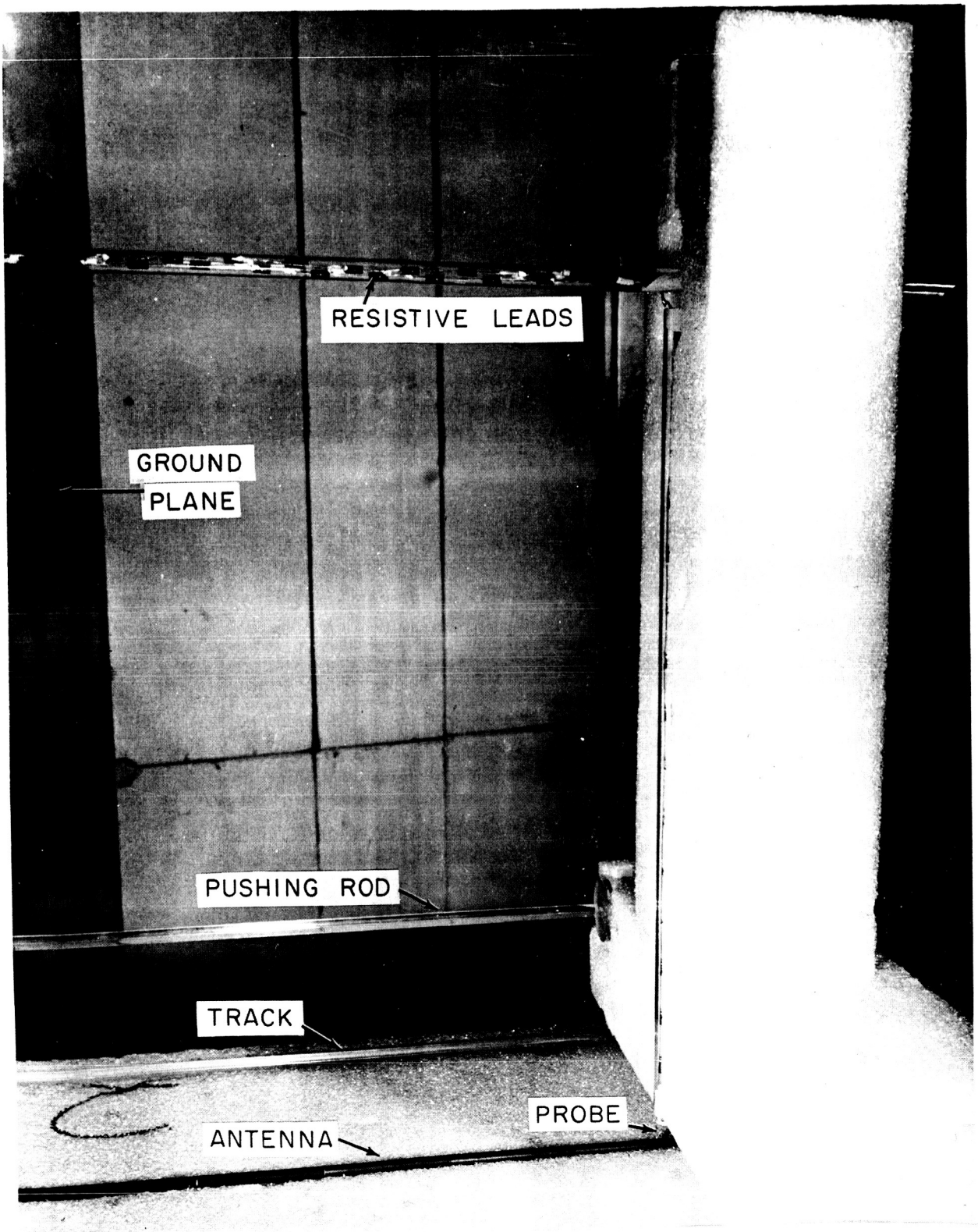

FIG. 5 THE EXTERNAL PROBE AND ITS SUPPORTING STRUCTURE

antenna and the diode does not vary more than 0.05 cm and the deviation of the probe from the center of the antenna can hardly be detected visually.

To check the performance of the resistors in the r-f field, the vertical section of the resistive wires has been put into a polyfoam-filled (ϵ_r = 1.04) slotted brass tube of 4.84 cm i.d. to form a lossy coaxial line. Measurement showed that the attenuation of the current on this transmission line was about 60 db per wavelength at 600 MHz. A similar test has been given to the horizontal section; the attenuation was found to be 40 db per wavelength at the same frequency. It is believed that the resistance of the leads is high enough in order not to disturb the field due to the antenna during measurement of current distribution.

The external probe was used to measure the current distribution on a brass monopole antenna and the result is compared with that measured by means of an ordinary internally connected shielded loop with a superheterodyne detection system. The loop of the external probe was kept close to the brass antenna so that the diode was about 0.1 cm above the antenna during the measurement. The resulting experimental data are plotted in Figs. 1 and 2, and the agreement between the two sets of data is in general good. The discrepancy is mainly at the current minima. In order to study the effect of the variation of the distance between the external probe and the antenna on the observed current distribution, the probe was deliberately moved vertically both ways by 0.05 cm which was the maximum possible distance deviation of the probe from the antenna as it

traveled along and above the antenna. It was observed that the signal varied in the range of 0.3 to -0.3 db at the current maxima and 0.8 to -0.3 db at the current minima. The difference between the two sets of readings observed with the two different probes at the current minima sometimes amounted to 2 to 3 db as seen from Figs. 1 and 2. The difference near the current null is attributed to the fact that the external probe has larger dimensions (1 cm × 1 cm) than the shielded loop (0.02 cm in diameter) so that the former responds to the averaged field at the current null which is larger than the field strength at that point. the in-ability of the external probe to detect accurately a current minimum is not a serious defect in the present case because for a resitive antenna the current distribution is expected to vary smoothly.

In plotting the experimental data, the mid-point of the diode in the external probe is arbitrarily referred to be the position of the external probe. But it is seen from Figs. 1 and 2 that the agreement is better if the anode end of the diode is chosen to be the reference point instead. Hence, in all following measurements, the position of the external probe is determined by the position of the anode end of the diode.

4. The Resistive Coating

The resistive antenna is composed of sections of dielectric rod coated with resistive paint. The dielectric rod is made of 1/4-inch plexiglass rod. The ends of each sections are machined so that sections can be screwed into one another after having been sprayed individually. Two brass ends are made

to fit each rod. They serve as a protection for the screw ends against resistive paint in the process of spraying and also as a good electrical contact for d-c resistance measurements. These brass ends are removed when the individual sections are connected together to become a resistive antenna.

The brass-ended plexiglass cylindrical rod is put on a lathe ready for spraying. After many tests, the resistive paint finally chosen was commercially called "Shielding Paint" (NO. RS-14, made by Micro-Circuits Company of Michigan). The choice was made because this paint can be thinned to be sprayed in a spraygun and still be adhesive, the resistance stays relatively constant after spraying, and the paint does not settle too quickly for uniform spraying along the rod.

The Shielding Paint is first thinned by adding an equal amount of solvent (Normal Butyl Acetate), then filtered through two overlapping disposable paint strainers with 60 x 48 meshes per square inch. The spray gun is clamped to the automatic feeder of the lathe. While being sprayed, the plexiglass rod is revolving at a speed of about 3 revolutions per second, the spray gun advances about 1 cm per second, the distance between the spray gun and the rod is kept at about 8 to 10 cm, and the nitrogen pressure feeding the spray gun is regulated at 12.5 pounds per square inch.

For obtaining d-c resistance in the vicinity of 6000 ohms per meter, two to four coats are enough; for resistance near 800 ohms per meter, as many as ten to twelve coats are needed. In addition to the number of coatings as a variable to control the resistance of the rod,

the distance between the spray gun and the rod can be adjusted to get the proper thickness of the coating. All other factors, such as the opening of the nozzle of the spray gun and the nitrogen pressure, are kept unchanged. Nevertheless, since the rate that the paint is sprayed also depends on the liquid level of the paint in the container of the spray gun, precise control over the resistance is found very difficult. Because of this difficulty, excessive coating is sometimes reduced by sanding. This is done with the coated rod revolving on the lathe and with the automatic feeder guiding the sand paper which is held by the hand. The sand paper has very fine (No. 320) grits and each sanding stroke increases the resistance of the rod only about 1 or 2 ohms out of about 100 ohms. Sanding is used only for the low resistance range (about 1000 ohms per meter) and to increase the resistance of the coated rod by not more than 20 percent. Under a microscope the sanded surface can be seen to be rougher than the unsanded surface, but in general the roughness is no more than 20 percent of the averaged thickness of the coating. The averaged thickness of the coating on the rod can be estimated as sliced samples are viewed under the microscope. Some of the results are listed in the following table:

Table 1

Thickness of the Coating and the Conductivity

Sample	Resistivity (ohms/meter)	Thickness (cm)	Conductivity (mho/meter)
1	703	0.004-0.005	1.78×10^{3}-1.42×10^{3}
2	793	0.0035	1.80×10^{3}
3	845	0.0035	1.69×10^{3}
4	960	0.0035	1.49×10^{3}

Table 1 (Continued)

5	997	0.0035	1.43×10^{3}
6	1025	0.003-0.004	1.63×10^{3}-1.22×10^{3}
7	1040	0.003-0.004	1.60×10^{3}-1.20×10^{3}
8	1220	0.0025	1.64×10^{3}

According to the above rough estimate of the thickness of the coating, the conductivity of the resistive paint can be put to be equal to 1.5×10^{3} mho per meter. For this conductivity the corresponding skin depths d_s are 0.043 cm at 900 MHz and 0.061 cm at 450 MHz. The internal impedance per unit length z^i of a conducting tube of outer radius c and inner radius b is, according to eq. (3), p. 356 of [8].

$$z^i = r_o \left(1 - \frac{b^2}{c^2}\right)\left(\frac{\bar{\beta}_1 c}{2}\right)\left[\frac{J_o(\bar{\beta}_1 c)\, Y_1(\bar{\beta}_1 b) - Y_o(\bar{\beta}_1 c)\, J_1(\bar{\beta}_1 b)}{J_1(\bar{\beta}_1 c)\, Y_o(\bar{\beta}_1 b) - Y_1(\bar{\beta}_1 c)\, J_1(\bar{\beta}_1 b)}\right] \tag{4}$$

where r_o is the d-c resistance of the tube and

$$d_s = 1/(\pi f \mu_1 \sigma_1)^{\frac{1}{2}}, \quad \bar{\beta}_1 = (1-j)/d_s \tag{5}$$

where f is the frequency; μ_1 and σ_1 are respectively the permeability and the conductivity of the conducting tube.

In the present case, $t = c - b \doteq 0.005$ cm, $c = 0.3175$ cm and $t < d_s$, so that (4) can be reduced to (6) :

$$z^i = r_o \quad \text{for } t \ll c \quad \text{and } t < d_s \tag{6}$$

Therefore the internal impedance of the coated rod at r-f frequency can be determined simply by measuring its d-c resistance. To sum up, in this experiment the coated rod is fabricated by repeatedly spraying resistive paint on the surface of a dielectric rod and by sanding, if necessary,

until its d-c resistance has the desired value of the internal impedance.

The uniformness of the coating in the circumferential or in the axial direction of the rod cannot be measured. However, with the rod revolving at the speed of 3 revolutions per second and the spray gun advancing 1 cm per second in the process of spraying, while the jet of the spray covers about 1 cm×1 cm area at the surface of the rod, it seems reasonable to believe that the rod should be uniformly coated in the circumferential direction. As to the question whether it is evenly coated along the axial direction of the rod, some test spraying has been done and the results are listed below. Each test sample consisted of two sections of dielectric rod joined together by brass ends. It was sprayed as one unit. The resulting resistivity of each section is listed in Table 2.

Table 2
Resulted Resistivity (in ohms/meter) for
Uniformness Test

Operation	Sample 1		Sample 2	
	section A 2.99 cm	section B 5.98 cm	section A 3.31 cm	section B 5.00 cm
first sprays	4780 (+4.8%)	4430 (-2.4%)	3080(+2%)	2980 (-1.3%)
second sprays	1640 (+3.8%)	1550 (-1.9%)	1450 (+2.1%)	1400 (-1.4%)
third sprays	735 (-3%)	769 (+1.5%)	907 (+1.2%)	886 (-0.8%)
sanding	793 (-4%)	845 (+2%)	997 (+2.2%)	960 (-1.5%)

In the above table the number in the parenthesis is the percentage of the deviation of the resistivity in the indicated section from the averaged resistivity of the two sections combined. According to the above result it seems that the coating of the rod is reasonably uniform in the axial direction.

The evenness of the coating in the circumferential and in the axial direction was also checked under the microscope and no significant unevenness was observed.

The resistivity of the coating does not become stable until about five days after the spraying, for resistivity near 1000 ohms per meter; it would take longer for thicker coatings and shorter for thinner coatings. The resistance in general drops 3 percent every day in the first few days after spraying. In order to save time, some of the coated rods have been put to use only one day after the spraying, without waiting for their resistances to become stable. However, almost all measurements for each antenna were completed within ten hours in order to minimize the effect of the changing resistivity.

Warning for those who want to obtain the resistive coating by following the foregoing procedure: The Butyl Acetate used as the thinner of the resistive paint is highly evaporative and flammable. According to the University Health Service, prolonged contact with the skin or breathing vapor or spray mist should be avoided, the spraying should be done directly in front of an adequate ventilating facility, and a mask with a proper air filter should be worn by the worker during the spraying.

5. Design of the Stepped Internal Impedance

From the previous description of the spraying process for obtaining the resistive coating and the criterion as well as the method of checking the resulting internal impedance, it is clear that it is not possible to make an antenna with an internal impedance per unit length that varies continuously according to a certain pattern such as that described in (1). In order to approximate the variation of the internal impedance of (1), the only possibility seems to be dividing the antenna into a certain number of sections each with a constant z^i at a value close to the z^i of (1) at the

corresponding place. The resulting variation of internal impedance will then be in the form of a step function that zigzags around the smooth curve of (1). If the number of steps is sufficiently large so that the discontinuity in the α - factor is small, it is believed that the step function variation of z^i made according to (1) will be a good realization of the theoretically required smooth variation of z^i described by (1).

The first design of an antenna with internal impedance varying like a step function is shown in Figs. 6 and 7. It allows z^i of the antenna to vary between two fixed values of α near $\alpha = 1$, except for the last section. The length of each section is then decreased, but an interesting feature of this design is that the total resistance of each section is a constant, excluding the last section. This design restricts the variation of α within a certain percentage for most of the antenna. Since the characteristics of the antenna are theoretically known to be not critically dependent on the parameter α, it was hoped that this design would simulate best the antenna with the continuous resistive loading assumed in the theory. Two antennas of this design have been built and tested and the result is described in the next section.

A second design for the step function variation of z^i used in this experiment is as follows. The antenna is simply divided into several sections of equal length, with the internal impedance of each equal to that corresponding to the center point of this section that is prescribed by (1), as it is shown in Fig. 8. This makes the deviation of α from 1 larger away from the driving point than near it. However, the deviation of α from 1 should have less effect away from the driving point than that near it, it is

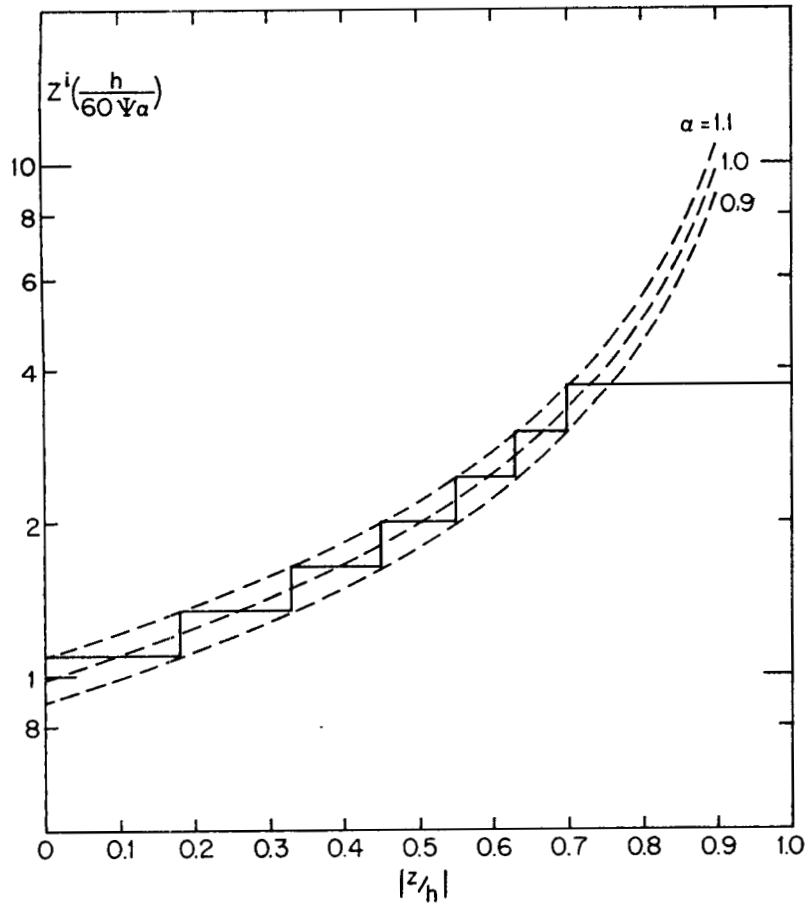

FIG. 6 DESIGN OF Z^i (ANTENNA NO. 2)

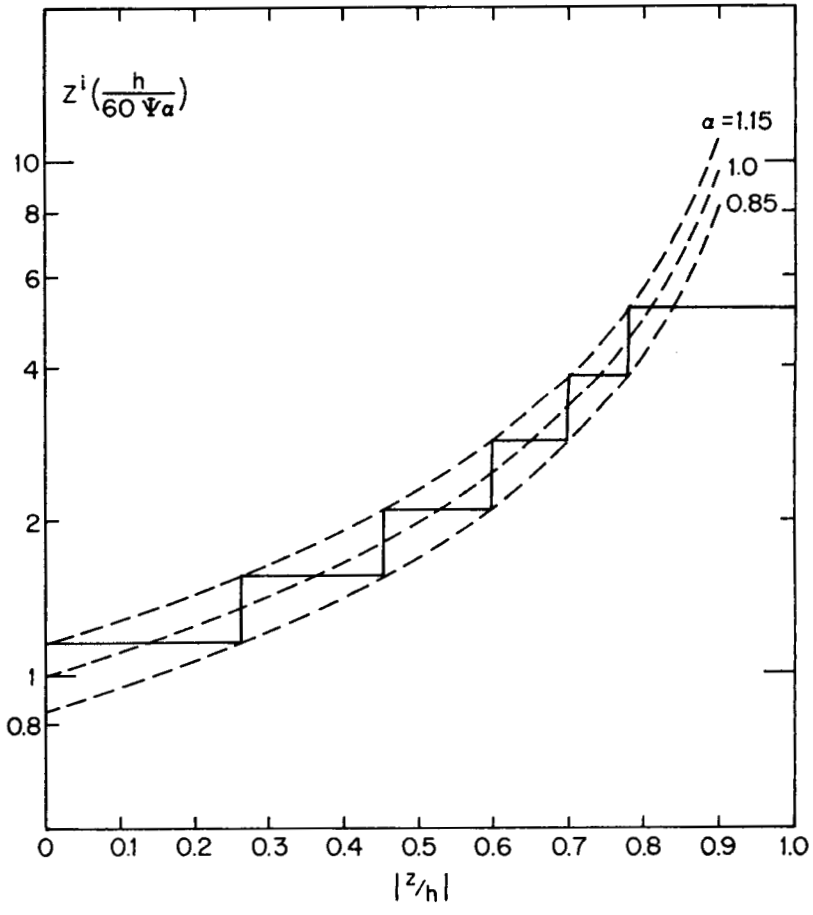

FIG. 7 DESIGN OF Z^i (ANTENNA NO. 3)

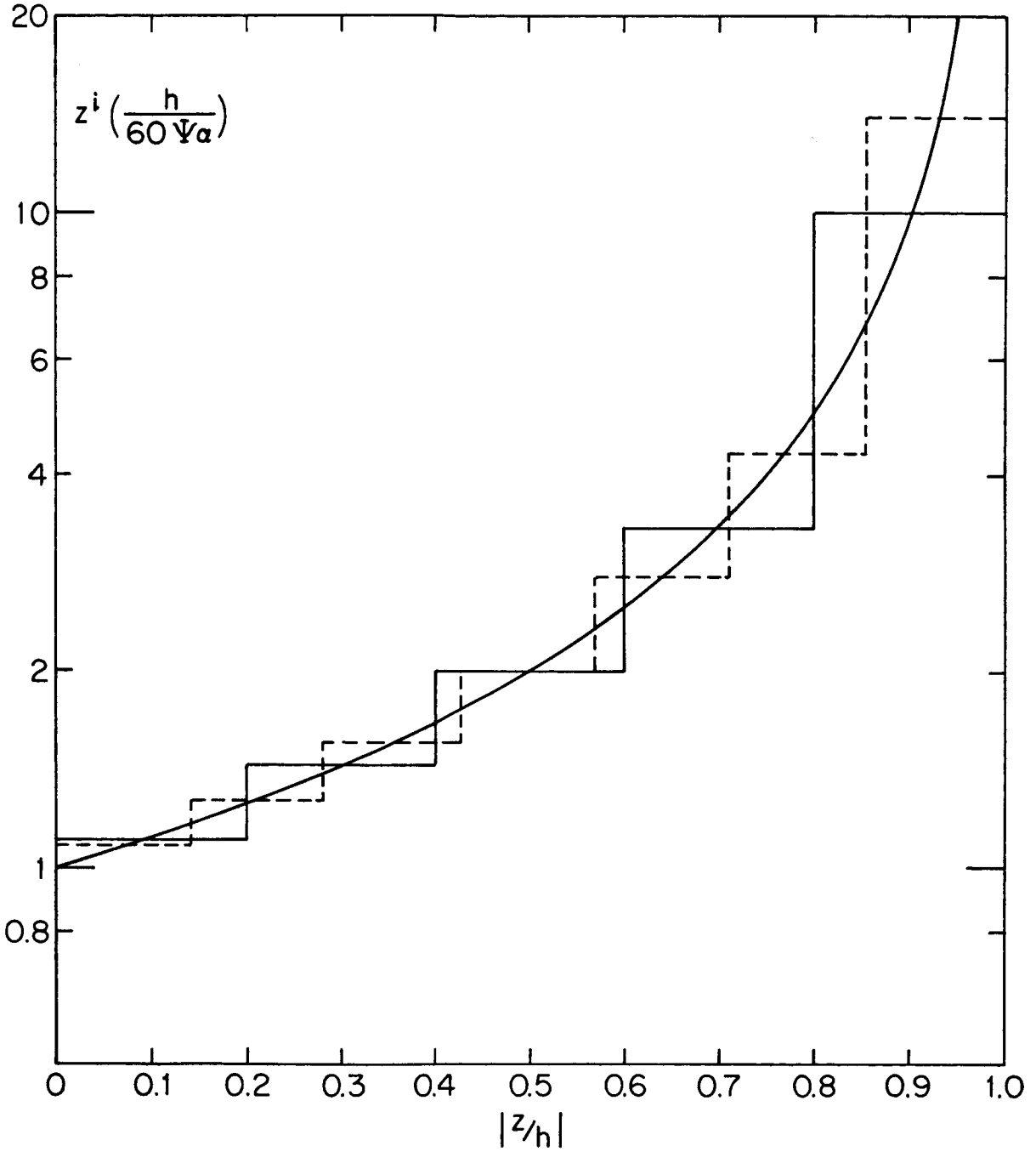

FIG. 8 DESIGN OF Z^i (ANTENNAS NO. 1, 4, 5, 6 & 7)

suspected that it is not necessary to keep fluctuations of a away from the driving point to the same percentage as that near the driving point as it is done in the first design. A seven-step and several five-step antennas with this design have been built and tested and the result is described in the next section.

6. Measured Current Distributions and Input Admittances

Seven monopole antennas were built for the measurement of the current distribution and the input admittance in the frequency range of 450 to 900 MHz. The lengths of the antennas are equal to 50.0 $\pm$0.5cm and the internal impedance per unit length of each antenna has been made according to either of the two designs described in the preceeding section. Specifications of these antennas are listed below in Table 3.

Table 3
Specifications of the Antennas

Antenna No.	$a\Psi$	Descriptions
1	4.1	5 equal-length sections (Fig. 8)
2	6.0	7-piece (Fig. 6)
3	6.0	6-piece (Fig. 7)
4	6.0	5 equal-length sections (Fig. 8)
5	6.0	7 equal-length sections (Fig. 8)
6	5.3	5 equal-length sections (Fig. 8)
7	7.0	5 equal-length sections (Fig. 8)

The value of $a\ \Psi$ refers to the symbol used in (1) and therefore it determines the level of z^i on the antenna.

Antenna No. 1 was intended to be put into a slotted brass tube of inner radius b to form a coaxial-line-like structure. If the current on the inner conductor (the resistive "antenna") is assumed to be equal in magnitude and opposite in phase to that on the outer conductor (the brass tube), which is approximately correct, the current distribution along this structure should be more accurately described by the zero-order theory than that of an antenna. The proportionality constant Ψ defined in (3) for the "coaxial line" is equal to $2 \log (b/a)$, which does not involve the frequency at all. The inner radius of the slotted brass tube used in the experiment is 2.42 cm, which makes Ψ of the coaxial line equal to 4.06. Thus the α factor of antenna No. 1 is equal to unity, and the current distribution is expected to decay linearly, and the phase to progress linearly as described by (2). The experimental result is shown in Fig. 9, where the magnitude and the phase of the current have been measured by means of an ordinary shielded loop with superheterodyne detection. The agreement between the theory and the experiment is remarkably good. This antenna was first built and tested, the result of the measurement brightened the hope that the resistive coating and the step-function design of the internal impedance should work favorably in case of other antennas.

Fig. 10 through Fig. 15 show the results of the measurement of the current distributions and the input admittances of the other six antennas listed in Table 3. The current distributions are plotted normalized to the input admittance. The input admittances are plotted in the form $Y=G+jB$ where $j=-i$. For an antenna, the proportionality

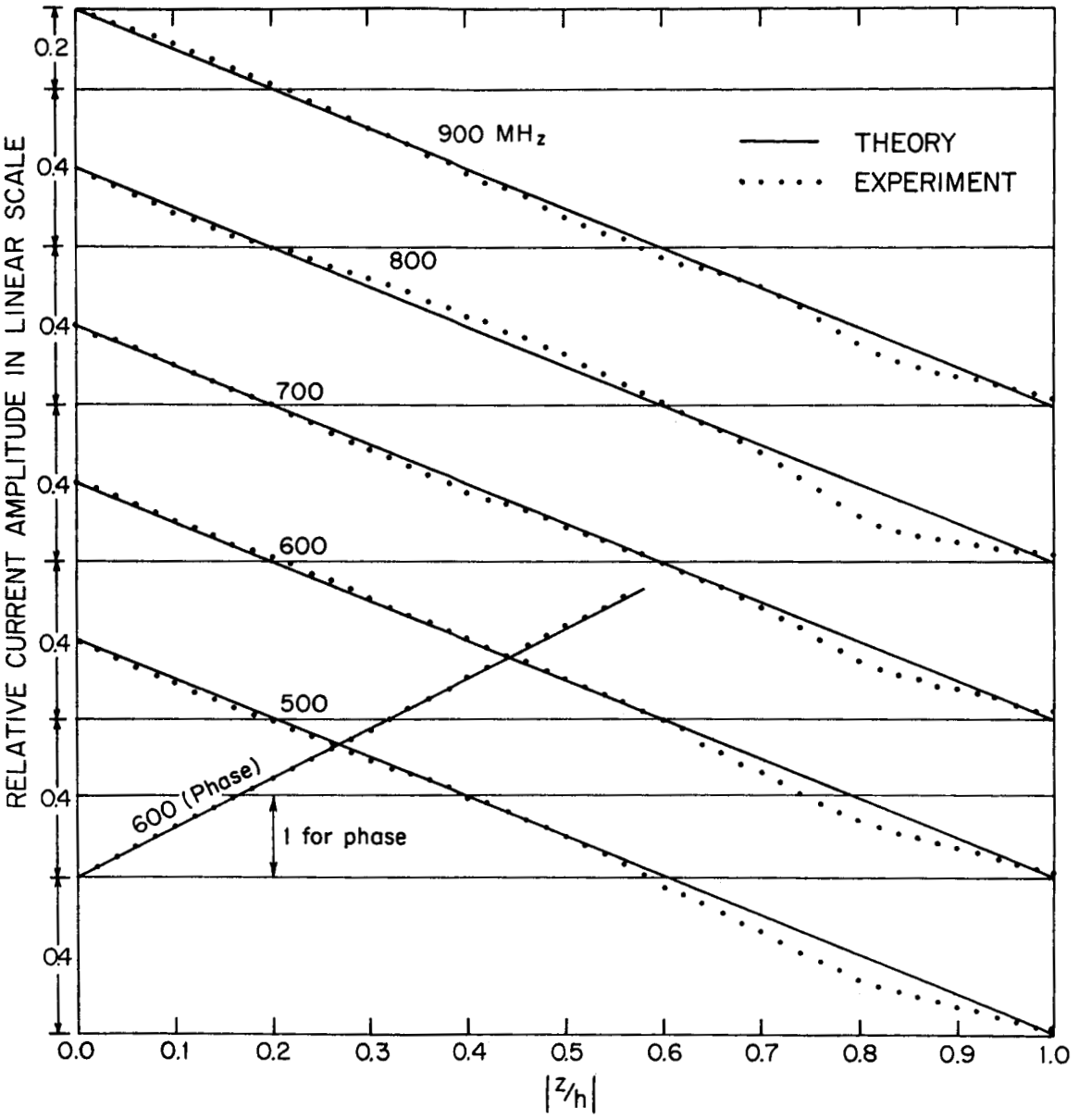

FIG. 9 CURRENT DISTRIBUTIONS ON ANTENNA NO. 1 IN COAXIAL LINE AT DIFFERENT FREQUENCIES.

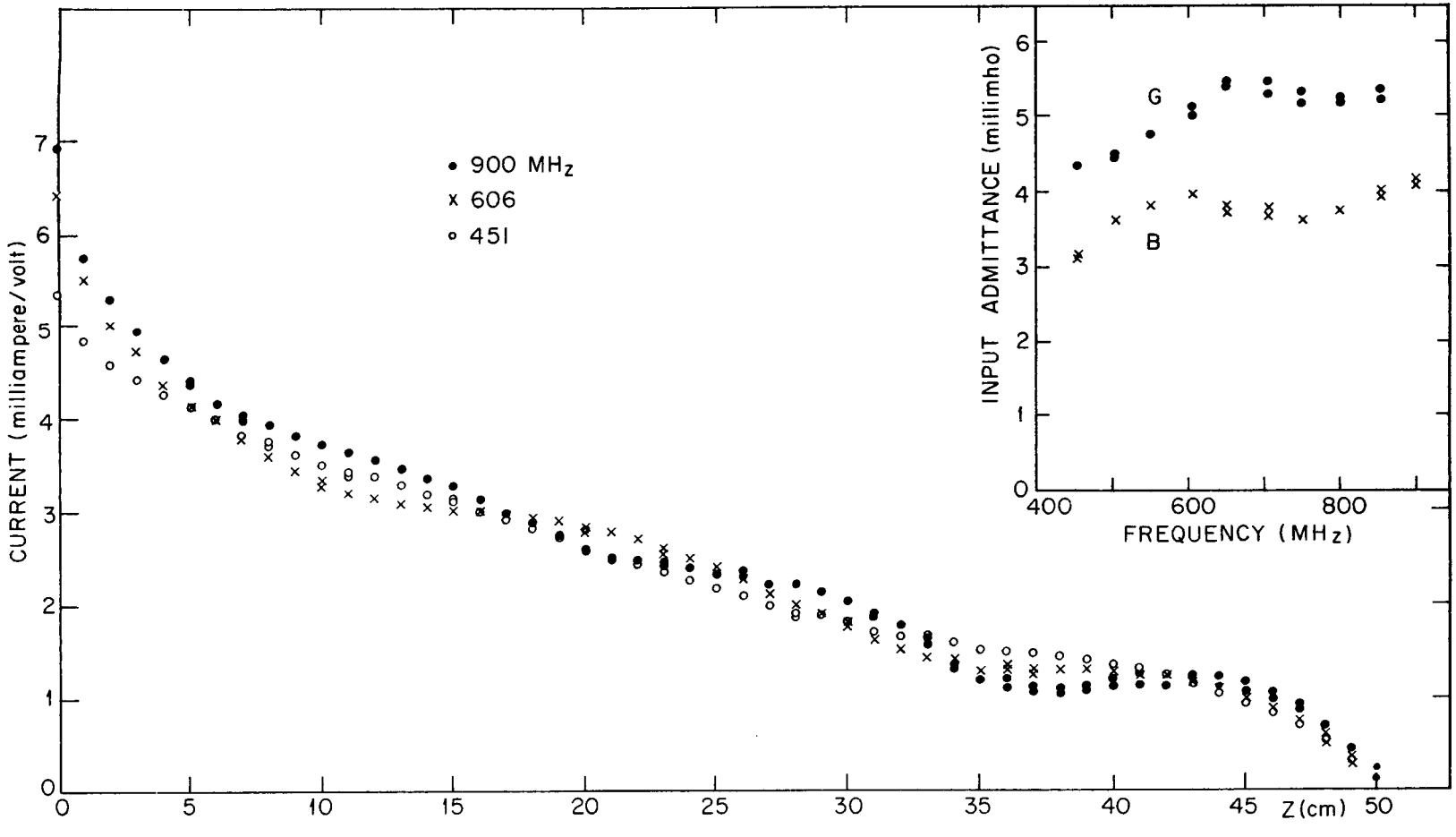

FIG. 10 CURRENT DISTRIBUTION AND INPUT ADMITTANCE OF ANTENNA No. 2

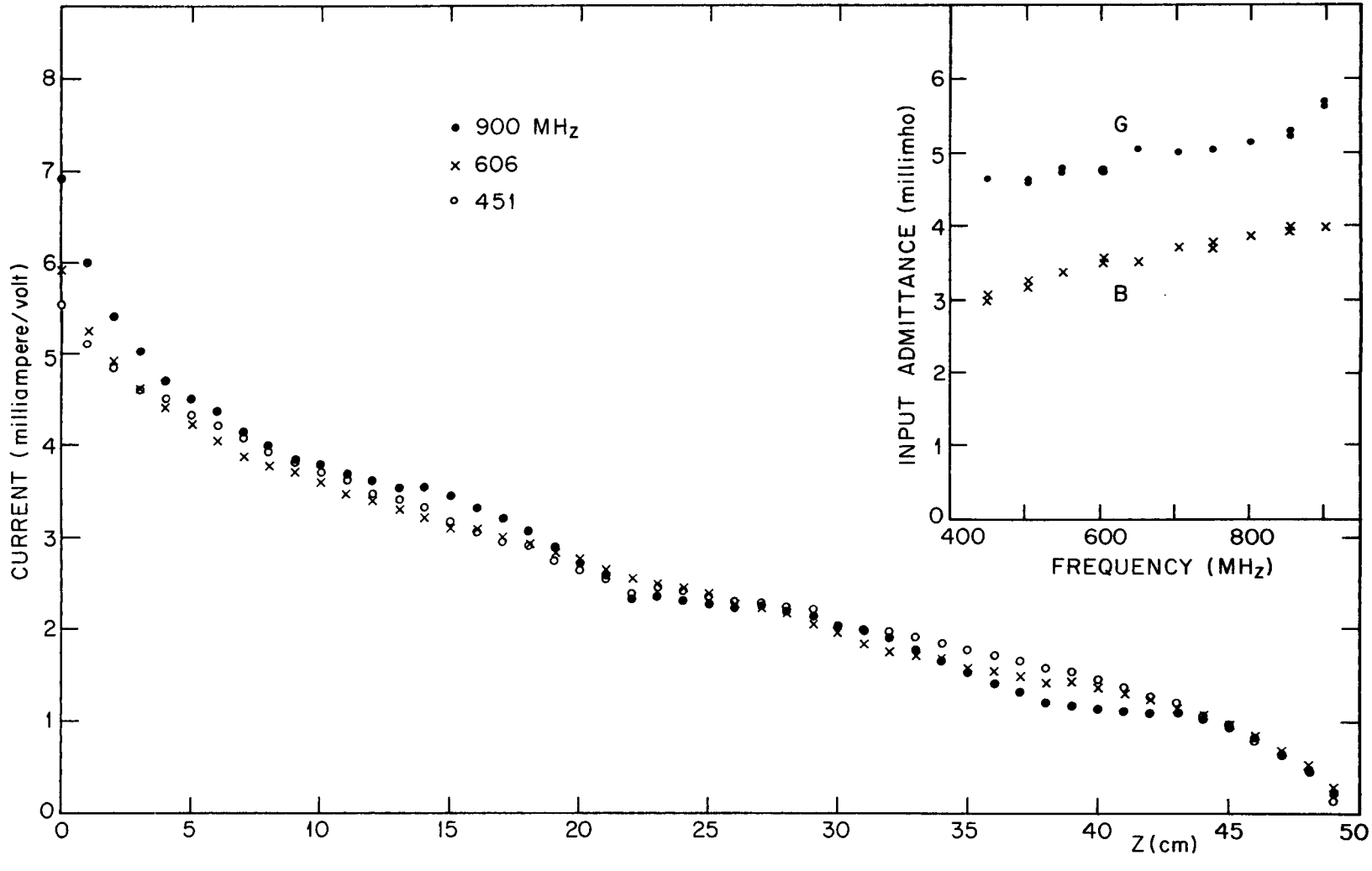

FIG. 11 CURRENT DISTRIBUTION AND INPUT ADMITTANCE OF ANTENNA No. 3

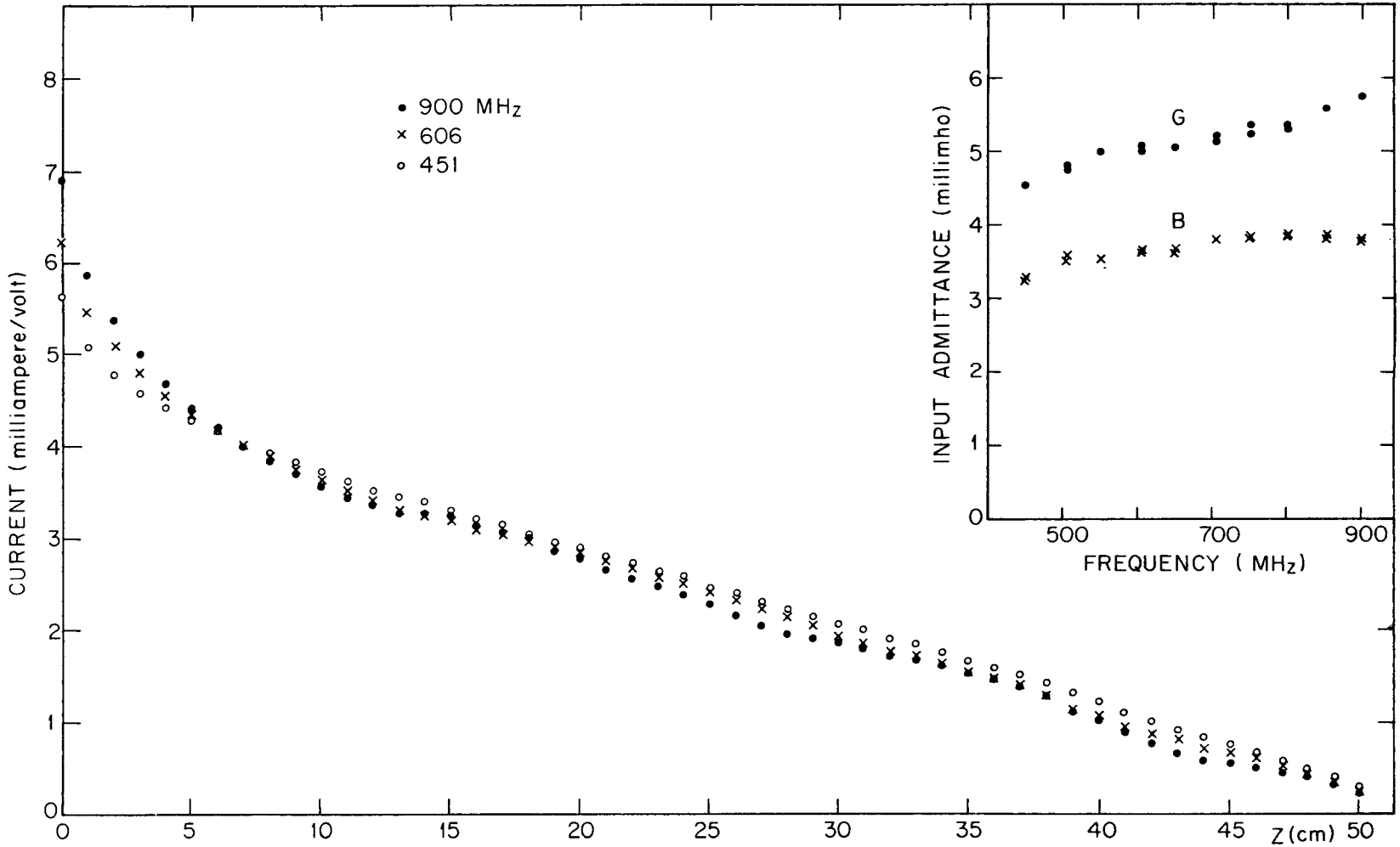

FIG. 12 CURRENT DISTRIBUTION AND INPUT ADMITTANCE OF ANTENNA NO. 4

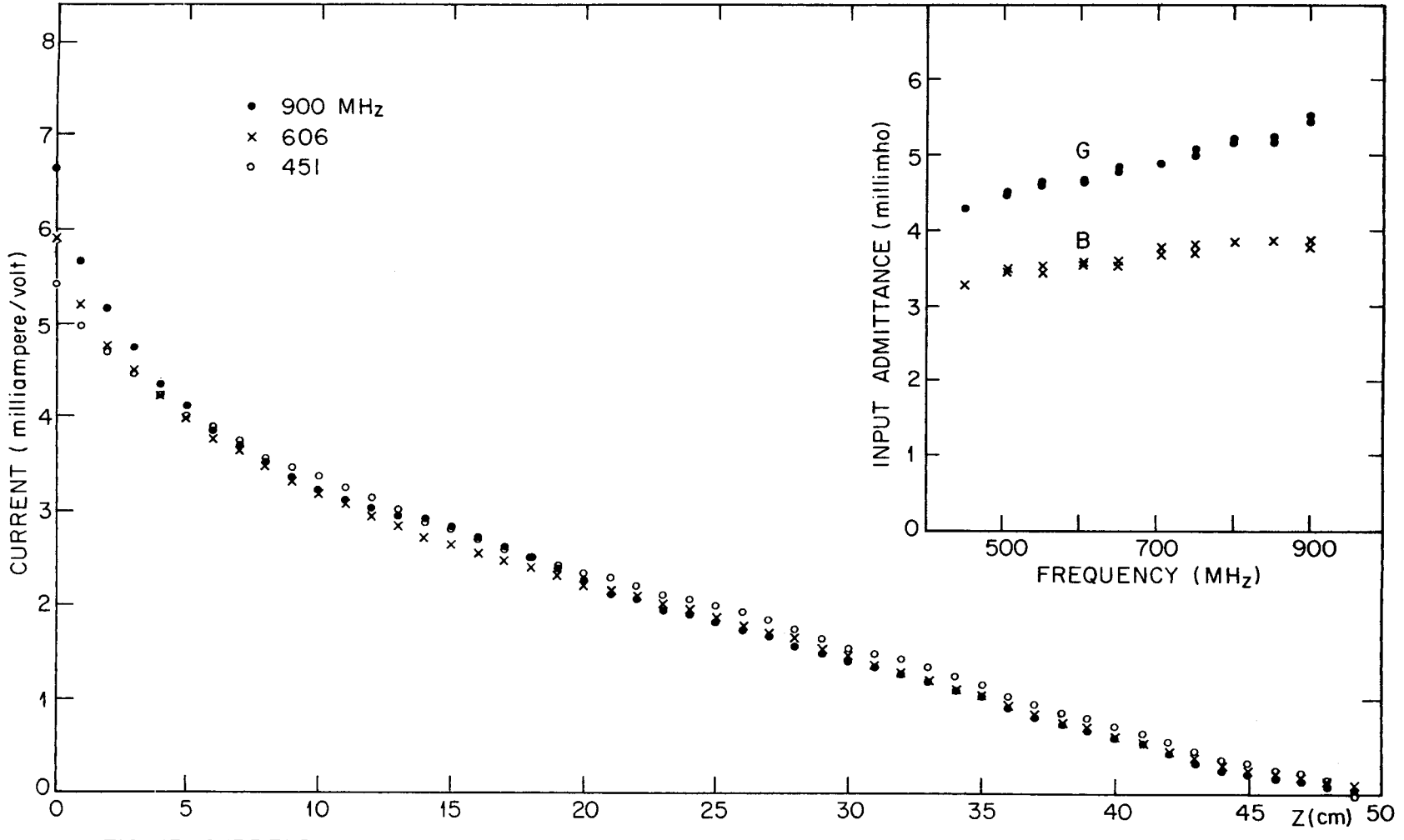

FIG. 13 CURRENT DISTRIBUTION AND INPUT ADMITTANCE OF ANTENNA NO. 5

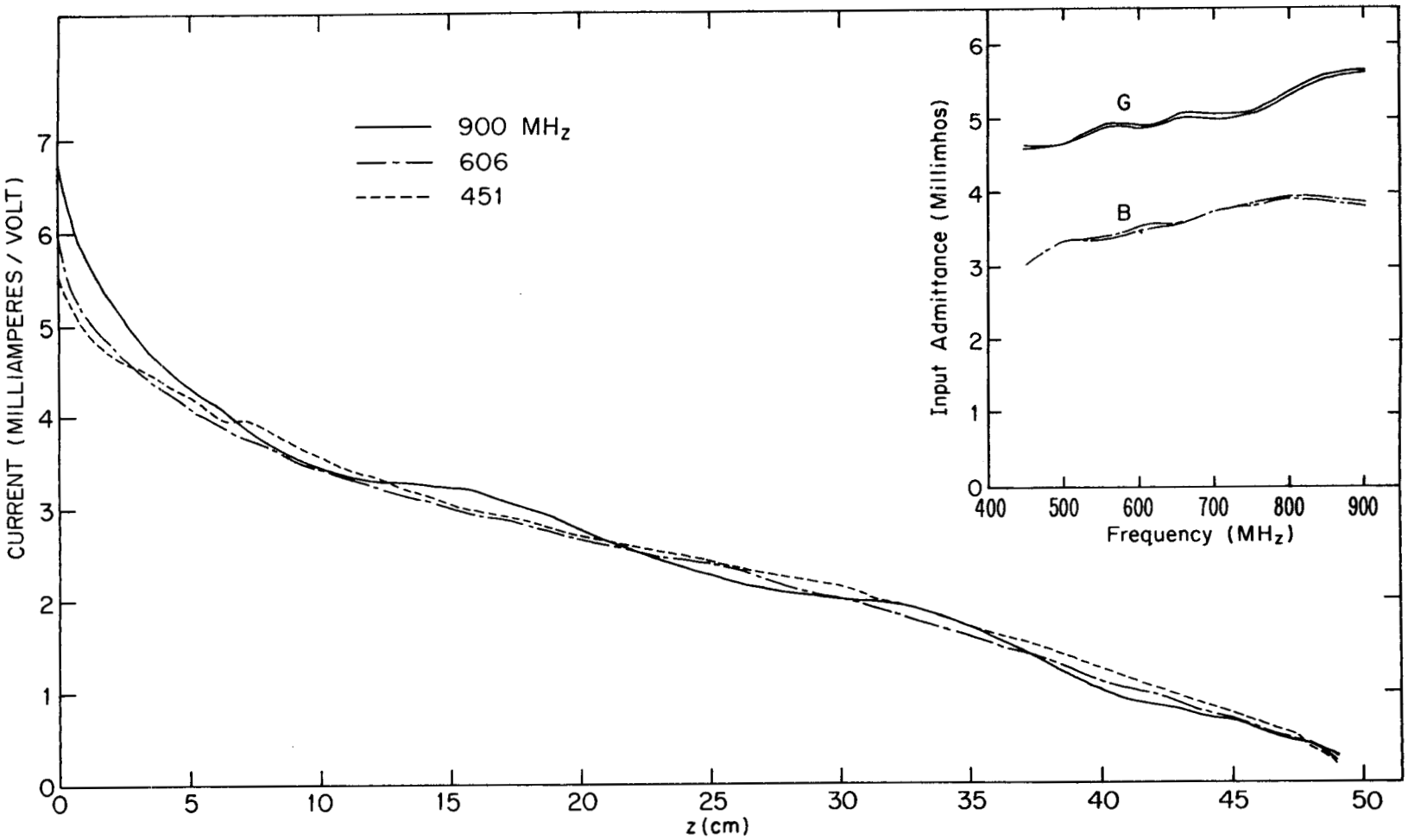

FIG. 14 CURRENT DISTRIBUTION AND INPUT ADMITTANCE OF ANTENNA NO. 6.

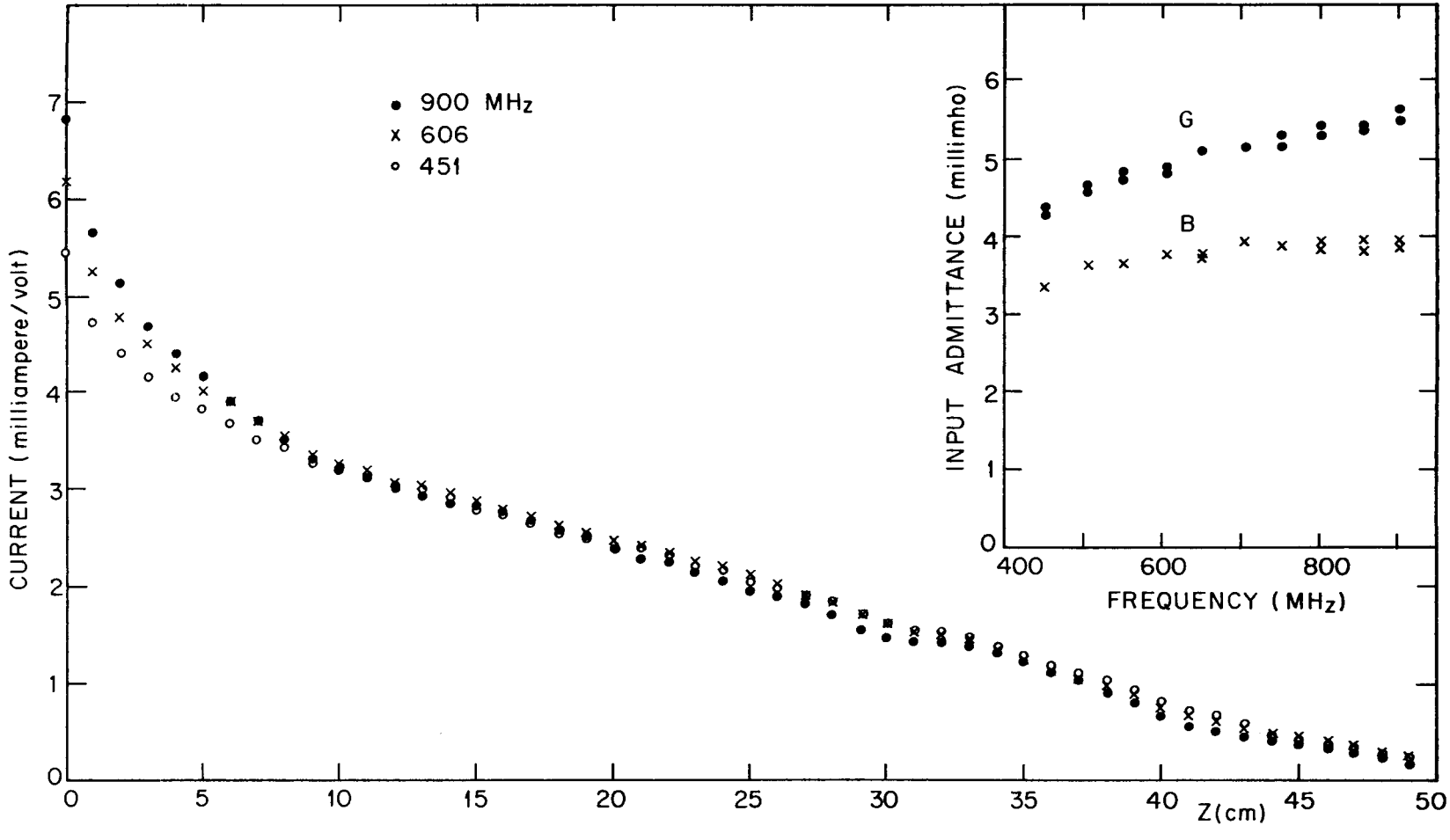

FIG. 15 CURRENT DISTRIBUTION AND INPUT ADMITTANCE OF ANTENNA No. 1

constant Ψ defined in (3) is equal to 6.06 at the frequency 600 MHz with the length of the antenna equal to 50.0 ± 0.5 cm and its radius equal to 0.3175 cm, which is calculated from the following formula: [Eq. 29, ref. 2]

$$\Psi = 2\left[\sinh^{-1}\frac{h}{a} - C(2ka,\ 2kh) - j\,S(2ka,\ 2kh) + \frac{j}{kh}(i-e^{-2jkh})\right] \qquad (7)$$

where $j = -i$.

therefore Ψ varies from 5.41 at 900 MHz to 6.57 at 450 MHz. For the z^i made so that $\alpha\Psi = 6.0$, as in the cases of No. 2, 3, 4, and 5 antennas, α varies from 1.11 at 900 MHz to 0.91 at 450 MHz. The fluctuation of α due to frequency is seen to be within the ambiguity due to the step-function variation of z^i .

From the experimental results, the current distributions can be seen to decay more or less linearly and remain relatively unchanged in shape as the frequency is varied. This agrees qualitatively with the theory. The input admittances stay rather constant in the frequency range, but quantitatively only its real part agrees with the theory. For comparison, the measured input admittances for all four antennas (No. 2, 3, 4, and 5) with different designs but with the same level of z^i are plotted in Fig. 16 together with the theoretical values, it is seen that although the designs vary, the measured input admittances are nevertheless within about 10 percent from each other. These measured input admittances are plotted together again in Fig. 16a for comparison with the theoretical value of the input admittance of an infinitely long antenna with the internal impedance equal to that near the driving point of the testing antennas. The agreement

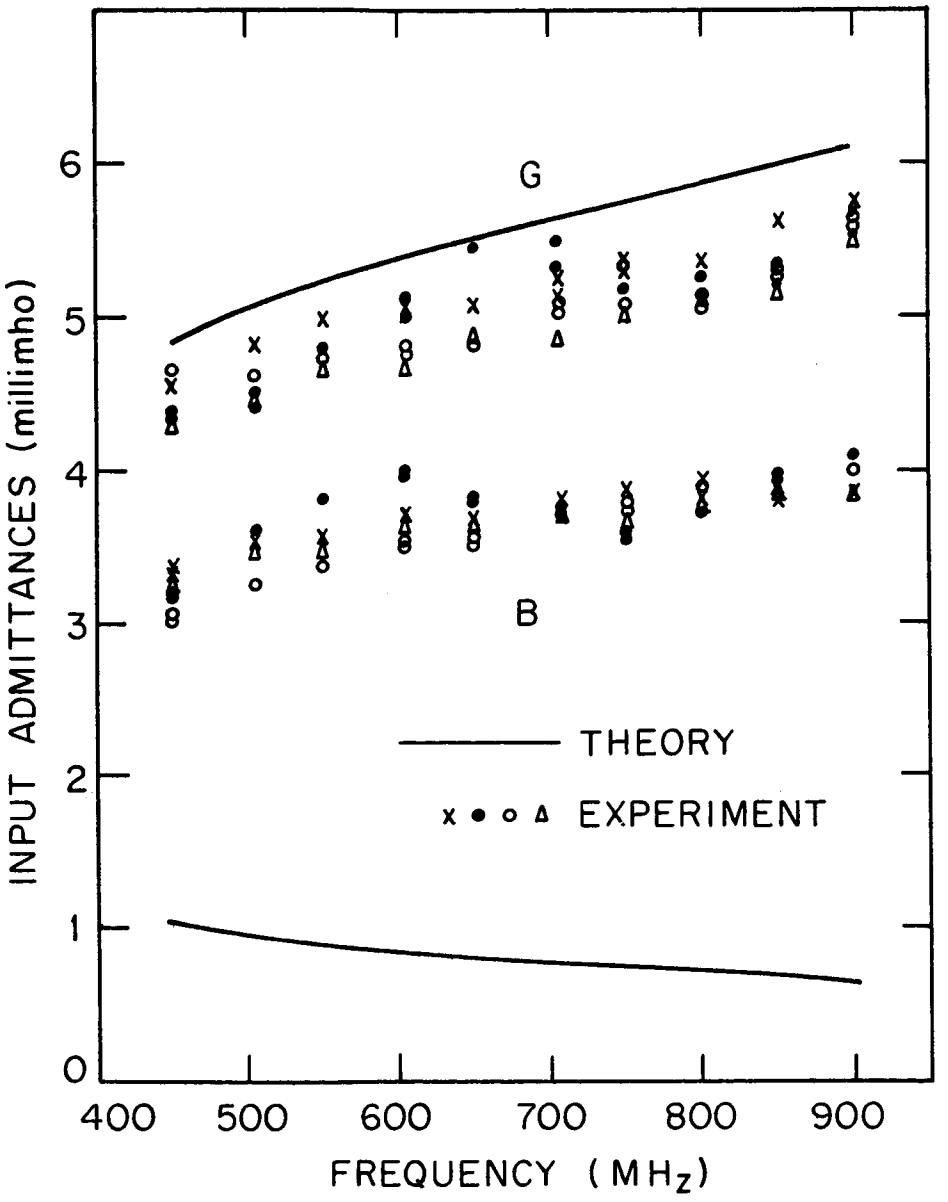

FIG. 16 INPUT ADMITTANCES OF ANTENNAS. No. 2, 3, 4 AND 5

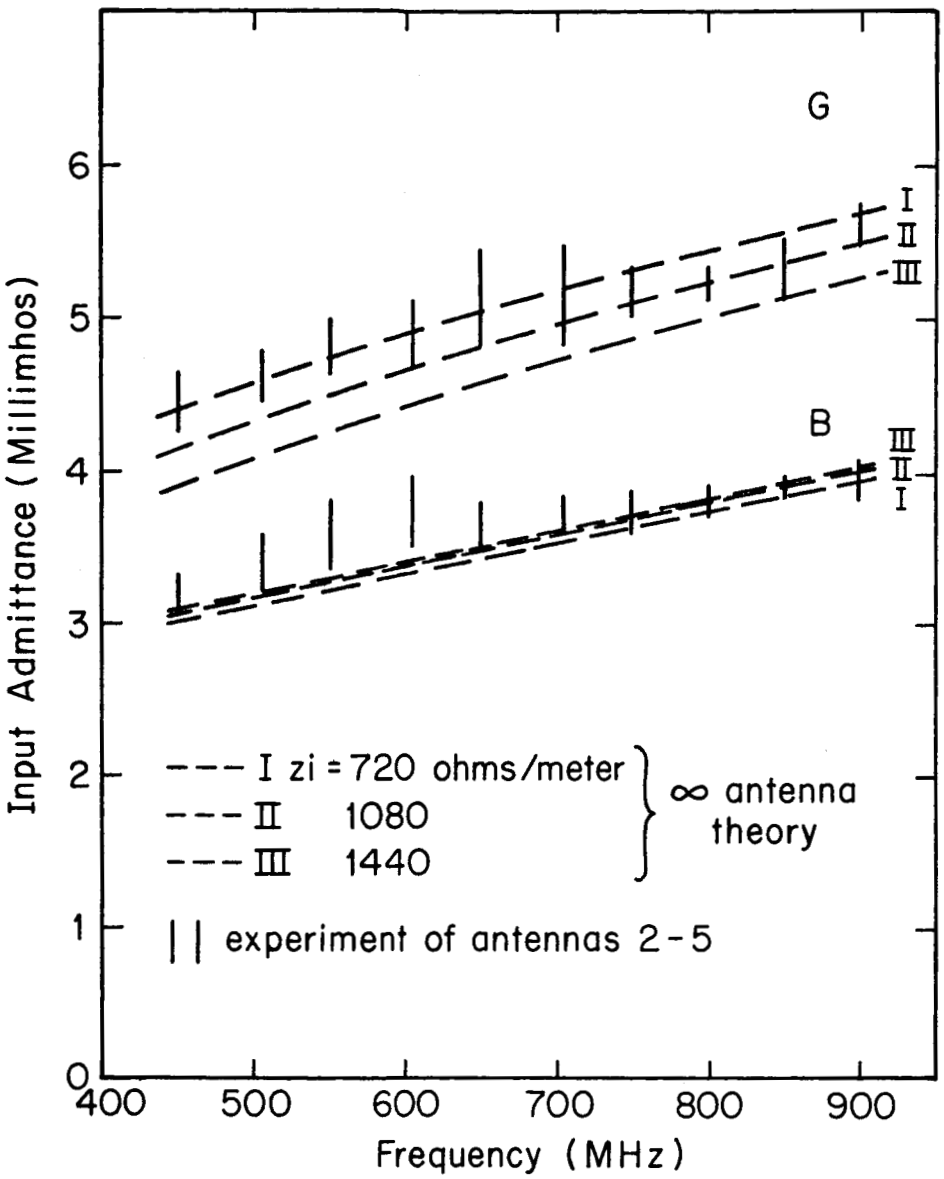

FIG. 16a INPUT ADMITTANCES OF ANTENNAS NO. 2, 3, 4 & 5 AND OF INFINITE RESISTIVE ANTENNA.

between them is seen to be remarkably good . The significance of this phenomenon has been discussed in Section 8.

The experimental current distributions for antennas No. 4, 6, and 7 and their input admittances are plotted in Fig. 17. These antennas are built according to the same design but with different levels of z^i, as listed in Table 3. These antennas were put spearately into the brass tube to form a coaxial-line-like structure and the current distributions were measured by a conventional shielded loop in order to verify their impedance levels. The currents were found to decay most rapidly on the "antenna" with the highest level of z^i (antenna No. 7) while the decay was least rapid on the "antenna" with the lowest level of z^i (antenna No. 6). This is as it should be. The currents are shown in Fig. 18. However, when operated separately as antennas, the current distributions do not differ very much and their input admittances are found hardly different from one another. The insensitivity of the current and the admittance with respect to the parameter a has been anticipated theoretically, as can be seen from Fig. 8 of [3].

7. Radiation Field Patterns

The radiation field pattern of the resistive dipole antenna has been obtained theoretically [3]. The corresponding field pattern of a V-antenna, (assuming that the current distribution on the antenna is not changed when the two arms of the dipole antenna are folded to form a V-shaped antenna), is given below:

$$F_{total}(\phi, \psi) = F(\phi + \psi/2) - F(\phi - \psi/2) \quad \text{on the plane of the V} \qquad (8)$$

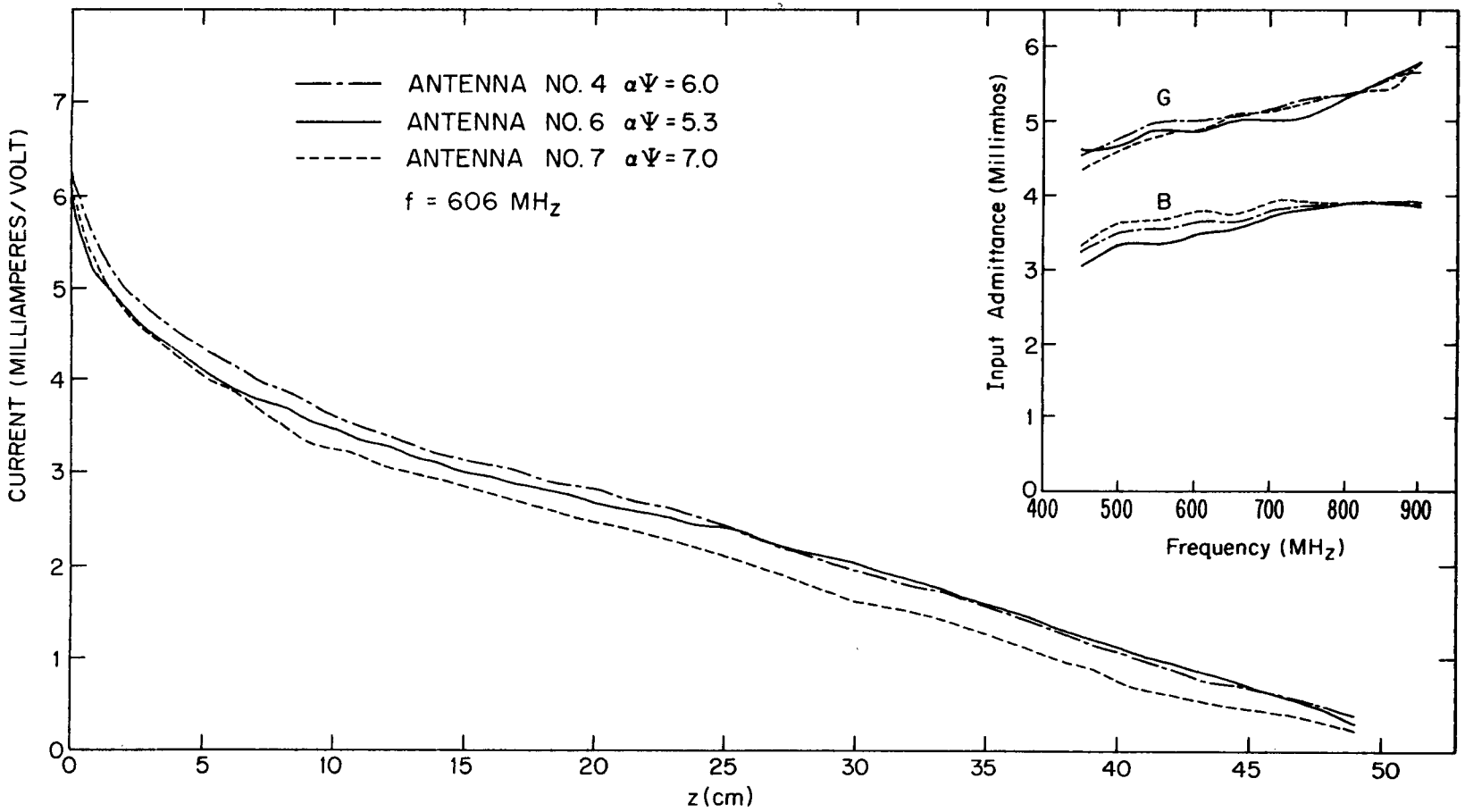

FIG. 17 CURRENTS AND ADMITTANCES OF ANTENNAS 4, 6, AND 7.

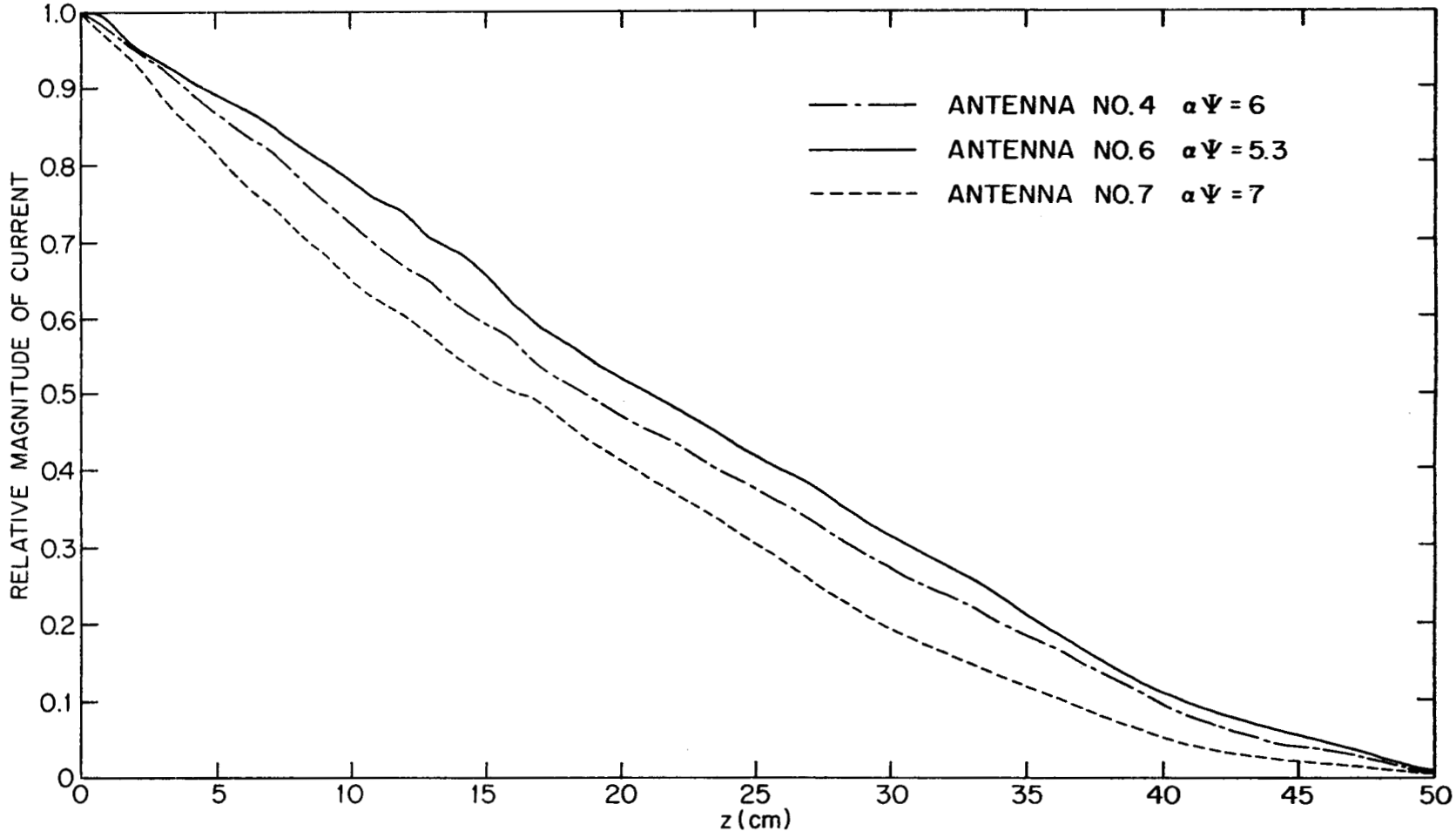

FIG. 18 CURRENT DISTRIBUTIONS OF ANTENNAS NO. 5, 6 AND 7 IN COAXIAL LINE

where

$$F(\phi) = \sin\phi \left[\frac{1+ ikh\,(1-\cos\phi) - e^{ikh(1-\cos\phi)}}{(1-\cos\phi)^2} \right] \tag{9}$$

where the angle ϕ is defined in Fig. 28, and ψ is the angle between the two arms of the V-antenna.

Traveling-wave V-antennas with each arm of the "V" loaded with a resistor have been studied both theoretically and experimentally by Iizuka [9], Duff [10], and Iizuka and King [11]. The existence of traveling waves on such an antenna has been verified experimentally and the directivity has been found to be very good. But the frequency bandwidth has not been studied experimentally.

Radiation field patterns of a dipole antenna with z^i for each arm varying in the form of five steps according to the second design described in Section 5 have been measured at frequency ranging from 900 to 490 MHz with the lengths of both arms equal to 50.5 cm and $\alpha\Psi = 6.0$. The measurement was done on the roof of the five-story high Gordon McKay Laboratory building in Harvard University. There was no higher building than this in the vicinity in the direction of the propagation of the incident wave during the time the experiment was done. The transmitting antenna with a parabolic reflector was placed on one side of the flat roof, aiming at the receiving antenna about 45 meters away which was erected on top of the penthouse located at the opposite side of the roof. The transmitting signal was modulated by 1 KHz square-wave audio signal. The arrangement of the set up is illustrated in Fig. 19.

The receiving antenna, for which the field pattern was to be measured, was placed on top of a semi-circular polyfoam table which had

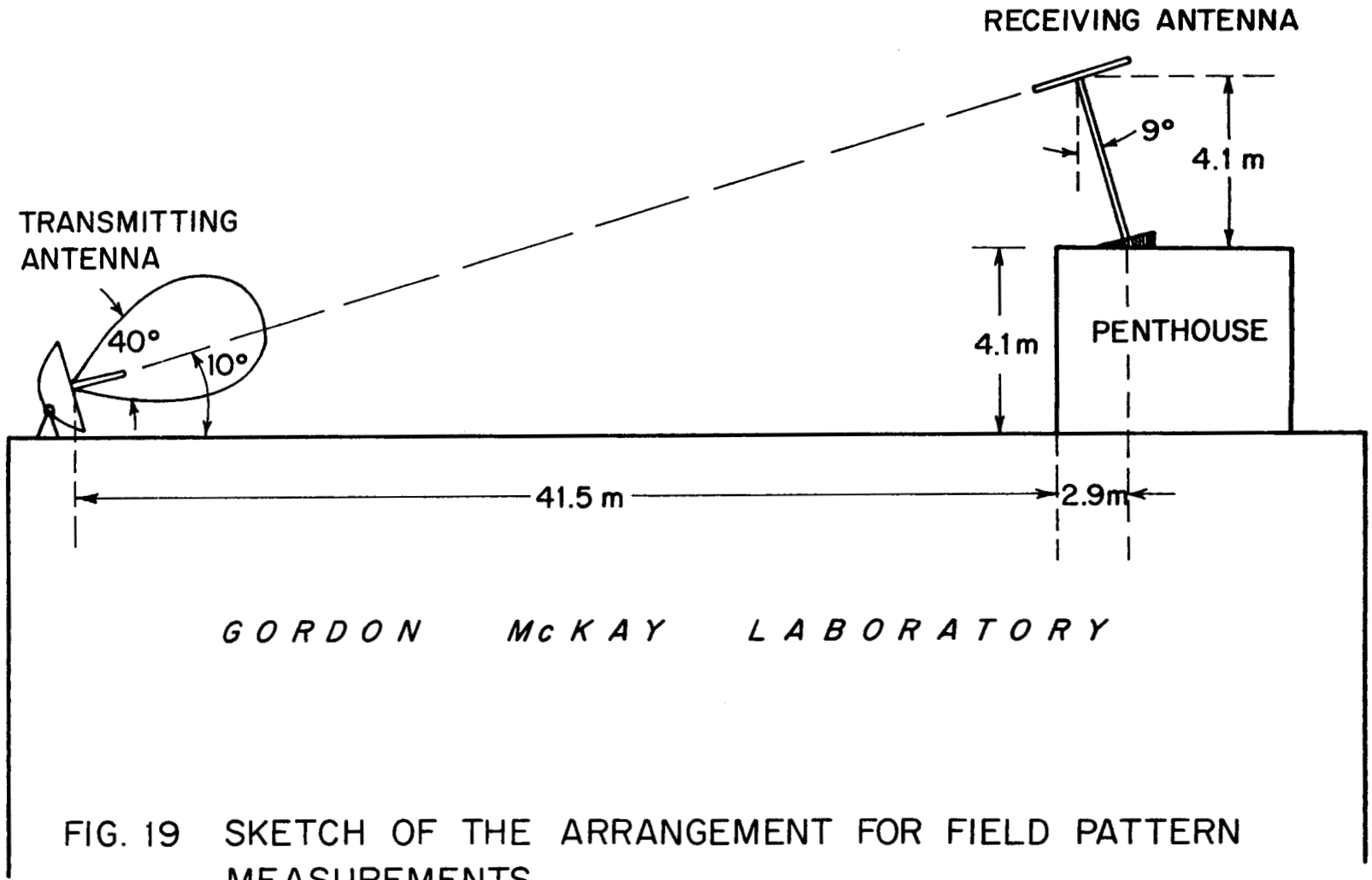

FIG. 19 SKETCH OF THE ARRANGEMENT FOR FIELD PATTERN MEASUREMENTS.

been cut radially to resemble a half wheel with ten spokes in order to reduce wind resistance. The polyfoam table was supported by a hollow wooden mast about 3 meters long, and which was in turn fastened on the turntable.

The signal picked up by the receiving antenna was fed through a two-wire line about 8 meters long that went through the hollow mast and leaded to the measuring equipments located in the penthouse. A section of two-wire line with a probe fixed at the neutral plane was inserted into the main two-wire line before it was terminated by a balun with the coaxial output of the balun connected to a crystal detector mount. The voltage probe in the neutral plane of the two-wire line was to monitor the unbalanced current.

The rectified signal was then fed to an automatic field pattern recording machine consisted mainly of a 1 KHz band-pass filter, audio amplifiers to drive the plotting pen, and synchronized motors to drive the turntable and the recording paper. A block diagram showing the measuring arrangement is shown in Fig. 20. The balun which converted the unbalanced termination of the coaxial line to a balanced load for the two-wire line is made by General Radio Company (Type 874 UB). The antenna field pattern recorder is manufactured by the Scientific-Atlanta, Incorporated of Georgia, with series APR 20 rectangular recorder, model CBA 21 crystal-bolometer amplifier, model PFA 32A pen function amplifier, series PC 1 positioner control unit, and series APR 20/30 Atlanta pattern recorder amplifier and power supply control.

The whole set up is similar to that used by Iizuka [9] except that

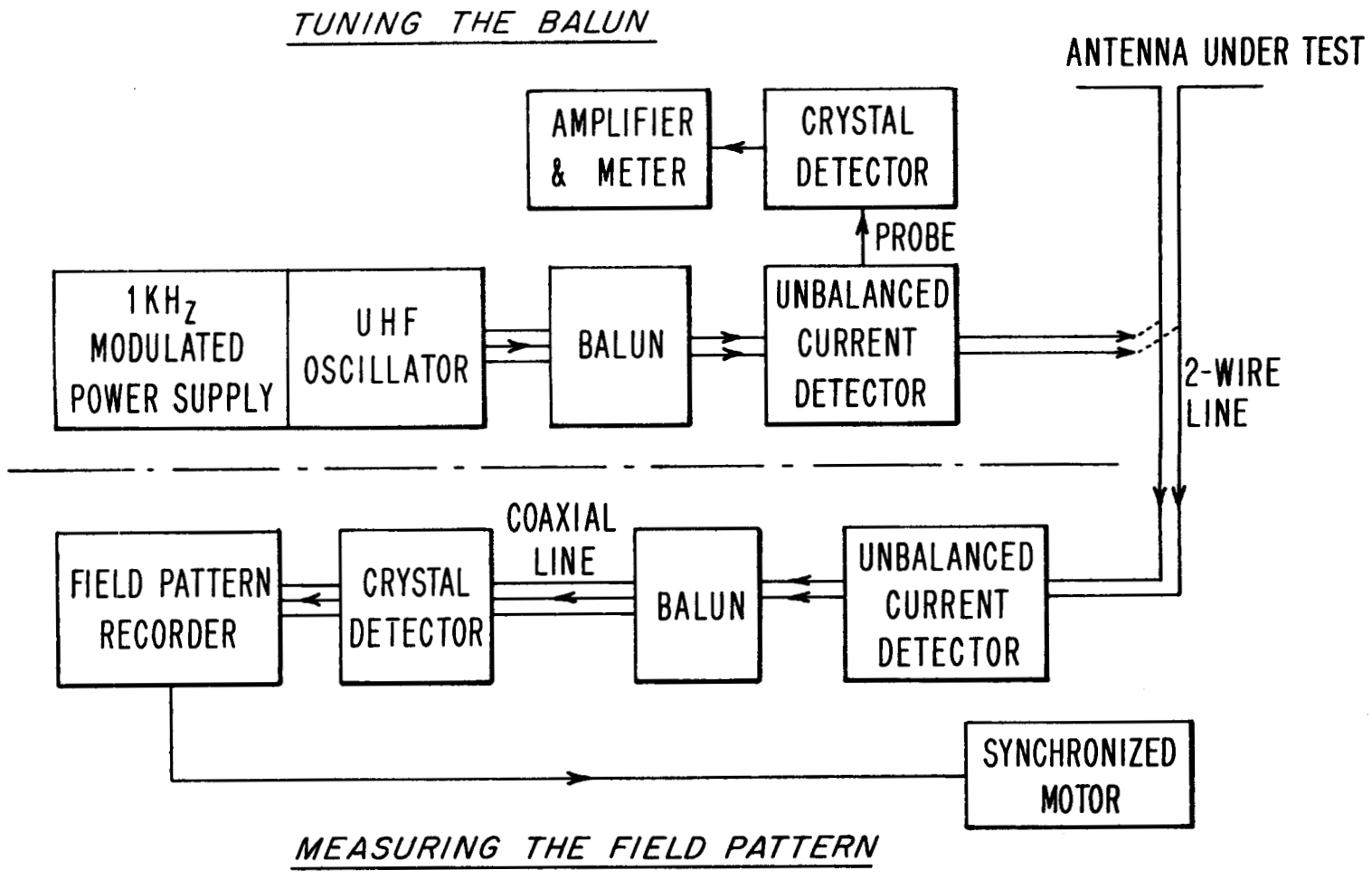

FIG. 20 BLOCK DIAGRAM OF THE FIELD PATTERN MEASURING SYSTEM AND THE TUNING PROCESS.

the unbalanced current monitor system and the height of the receiving antenna above the roof of the penthouse are different. Iizuka found that the fidelity of the measured field pattern was good if the antenna was placed higher or equal to 1.8 meters (or 3.5 wavelengths at 600 MHz) above the roof of the penthouse. In this experiment the antenna was elevated further to about 4.1 meters or 7 wavelengths above the roof at the lowest frequency. It is believed that for such a height the effect of the "ground" can be ignored.

The balun at the terminal of the two-wire line was tuned until the signal, picked up from the voltage probe at the neutral plane of the two-wire line, was minimum. At the same time the coaxial output port of the balun was fed by an oscillator at the desired frequency. This represented the balanced situation on the two-wire line. The "receiving" antenna was attached to the two-wire line when the balun was being tuned so that it acted as a transmitting antenna during the tuning process. A block diagram of the arrangement during the tuning process is shown in Fig. 20 .

The field pattern of a pair of ordinary brass dipole antennas with hemispherical caps at both ends was measured first and the result is plotted in Fig. 21 . The measurement was repeated for the balun so tuned that the signal from the unbalanced current monitor probe was successively 5 db, 10db, and 25 db higher than the minimum value. The 25 db unbalanced signal represented the most unbalanced situation of the two-wire line. It is seen that the unbalanced structure tends to affect the shape near the null of the field pattern but has less effect on the shape of the major lobe. This is understandable since for the unbalanced structure the transmission line

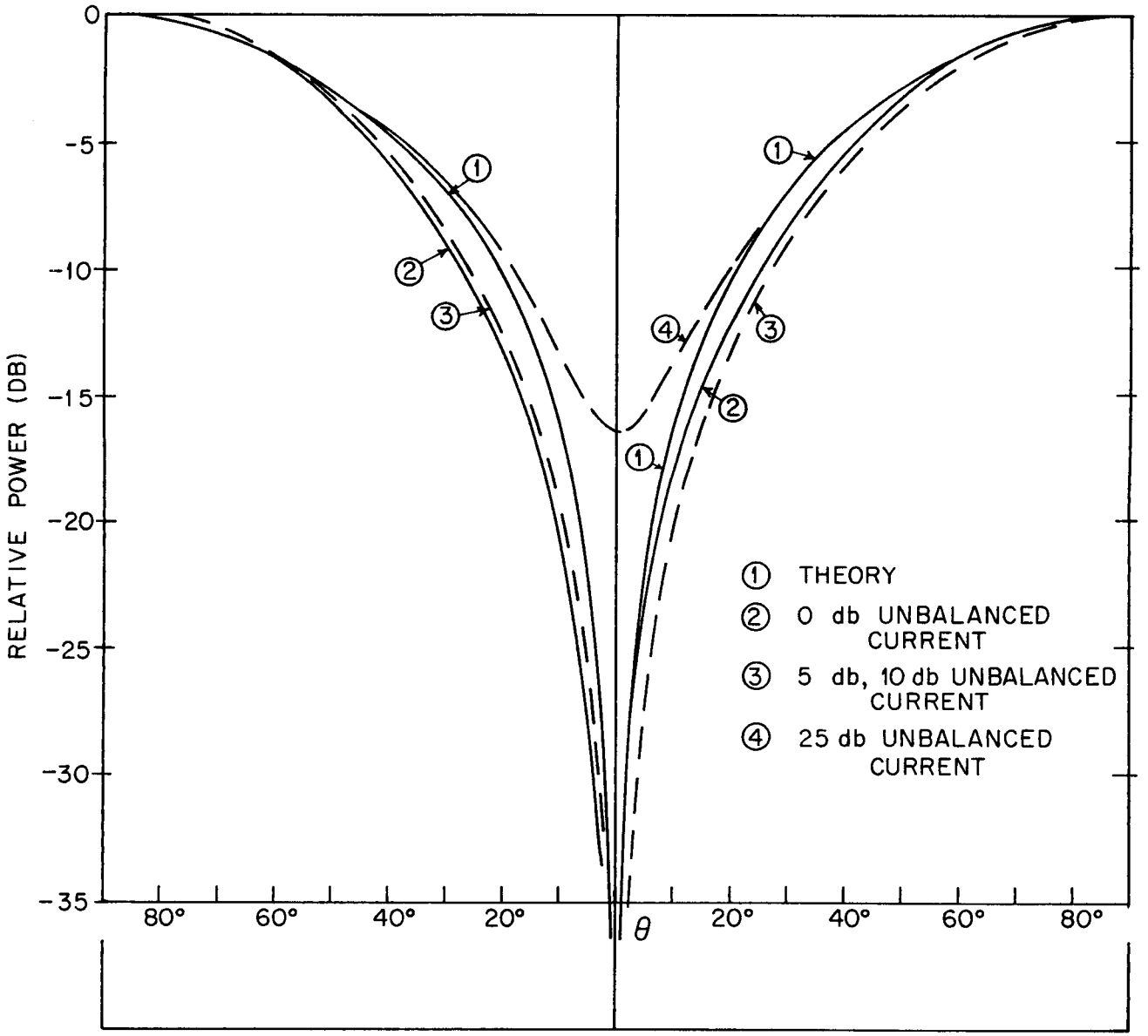

FIG. 21 FIELD PATTERN OF A BRASS DIPOLE ANTENNA AT 490 MHz, h = 12.5 cm

is also receiving a signal even at the null of the antenna field pattern.

The radiation pattern of a resistive dipole antenna was measured over the frequency range of 490 to 900 MHz. Each of the two arms of the dipole was built according to the second design described in Section 5 with five equal length sections. They were made as identical as possible and the current distribution of each was measured when they were put into the brass tube separately to form a coaxial line. Unfortunately, one of the arms was broken during the experiment and had to be replaced by another with less degree of similarity in z^i. The result of the current measurements for the latter two arms of the antenna is plotted in Fig. 22 and it can be seen that the current distributions on them are still very close to each other.

The measured radiation field patterns at five frequencies are plotted respectively in Figs. 23 through 27, together with the theoretical field pattern which, for simplicity, are based on the formula for $a = 1$. The agreement between the theory and the experiment is in general good.

The two arms of this dipole antenna were folded down to form a 90° V-antenna and its field pattern was measured over the same frequency range. The results of this experiment are shown in Figs. 28 through 32, where the theoretical curves are also presented. The agreement between the measurement and the theory which is calculated after (8) is found to be good. The front-to-back ratio of the 90° V-antennas are found to be more than 14 db and the major lobes are at least 7 db higher than any minor lobes for the frequency range of 490 to 900 MHz. The 6-db beam width of the main lobe decreases from 59° to 45° as the frequency changes from

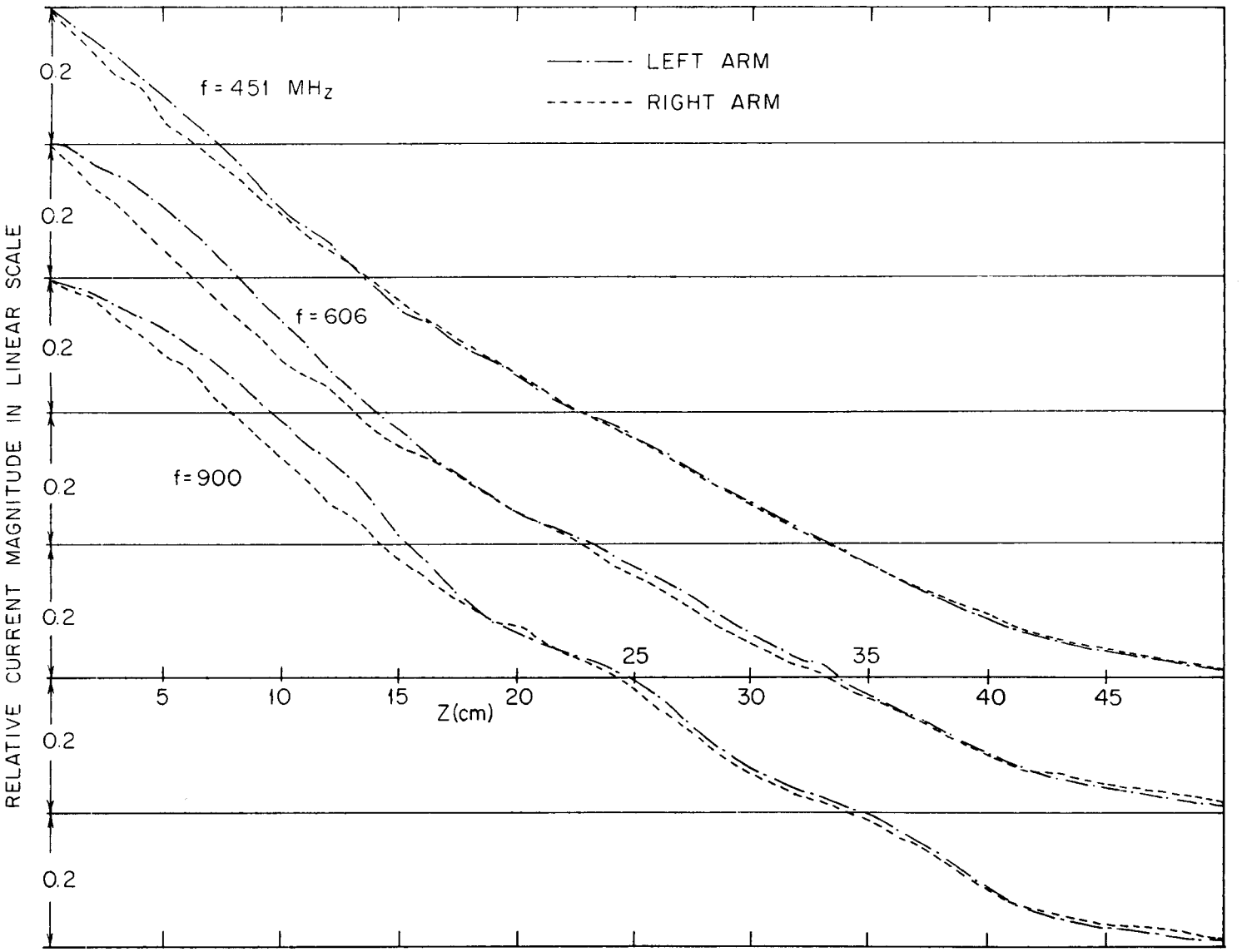

FIG. 22 THE CURRENT DISTRIBUTION ON THE TWO ARMS OF THE DIPOLE ANTENNA IN COAXIAL LINE SEPARATELY.

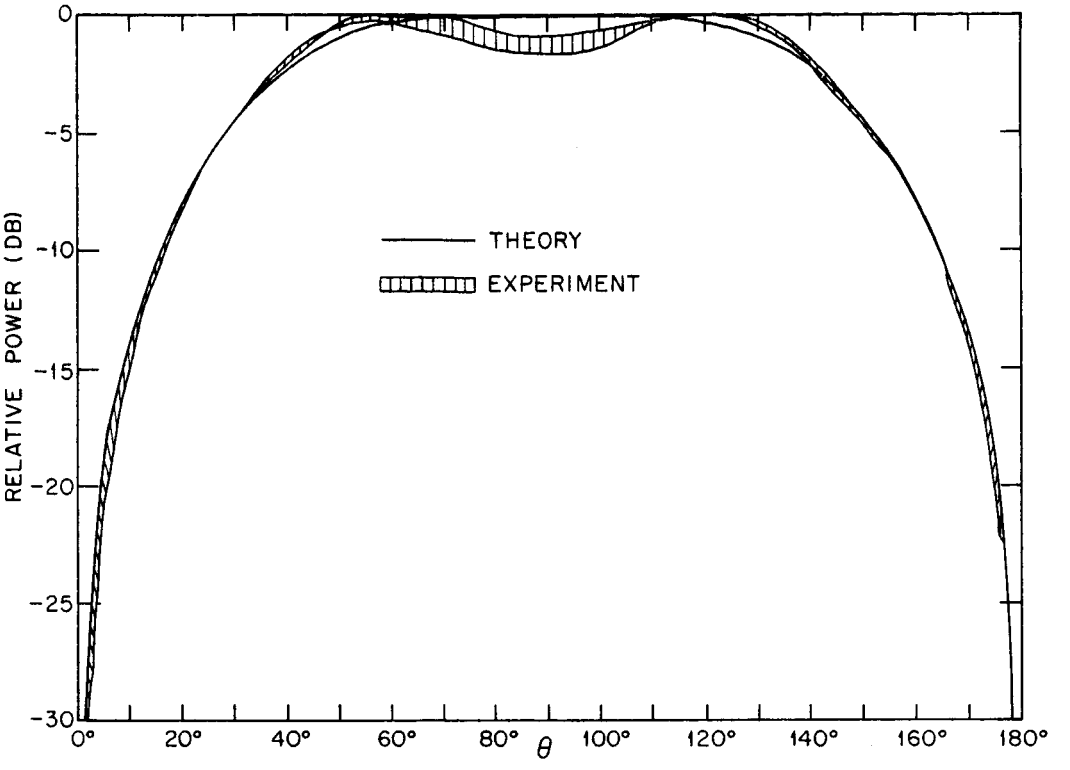

FIG. 23 FIELD PATTERN OF RESISTIVE DIPOLE ANTENNA AT 490 MHz

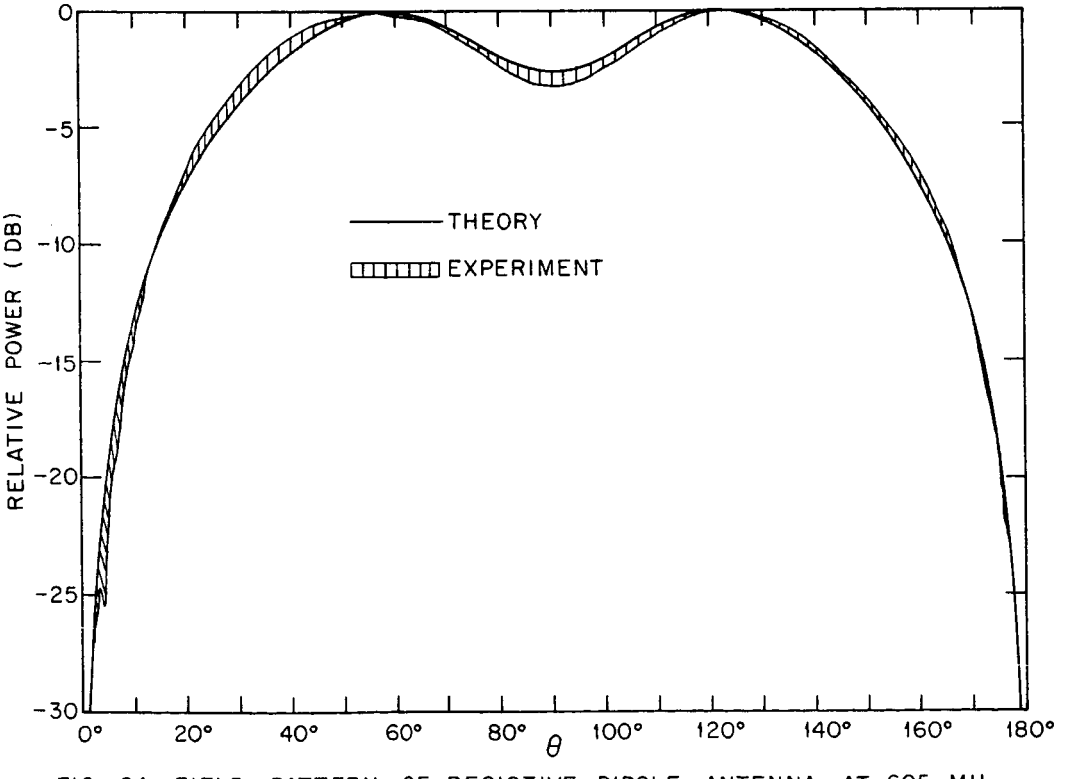

FIG 24 FIELD PATTERN OF RESISTIVE DIPOLE ANTENNA AT 605 MHz

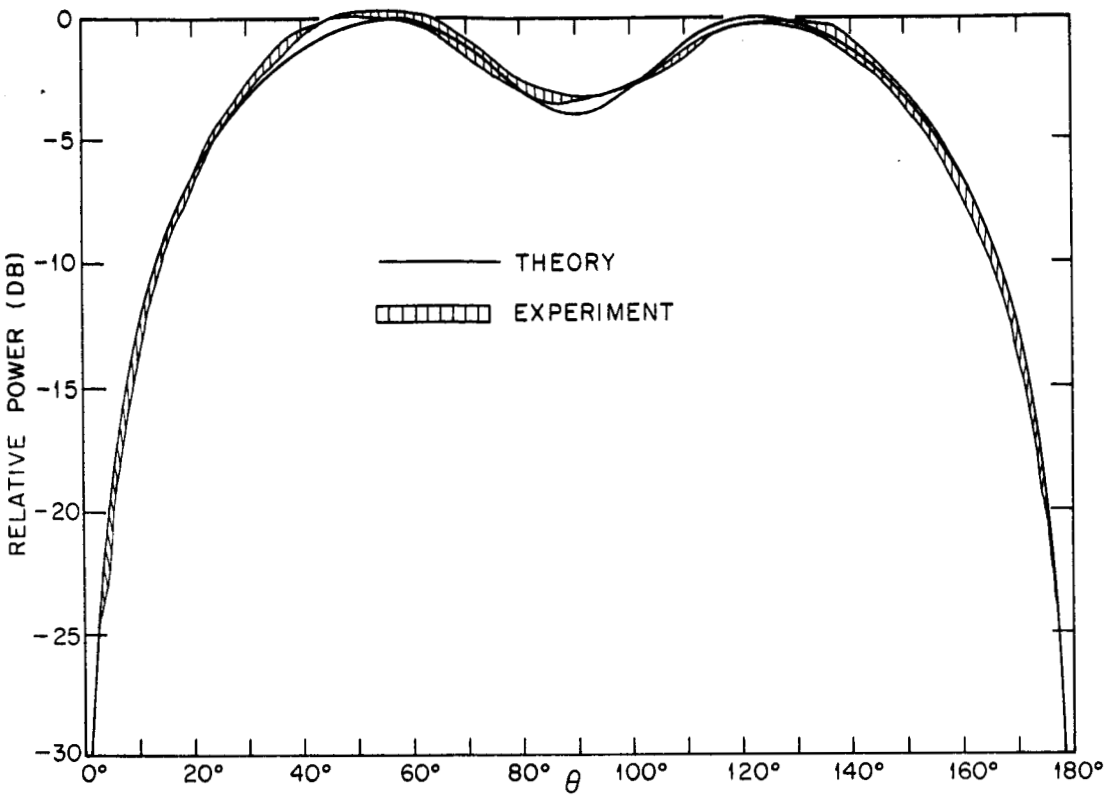

FIG. 25 FIELD PATTERN OF RESISTIVE DIPOLE ANTENNA AT 705 MHz

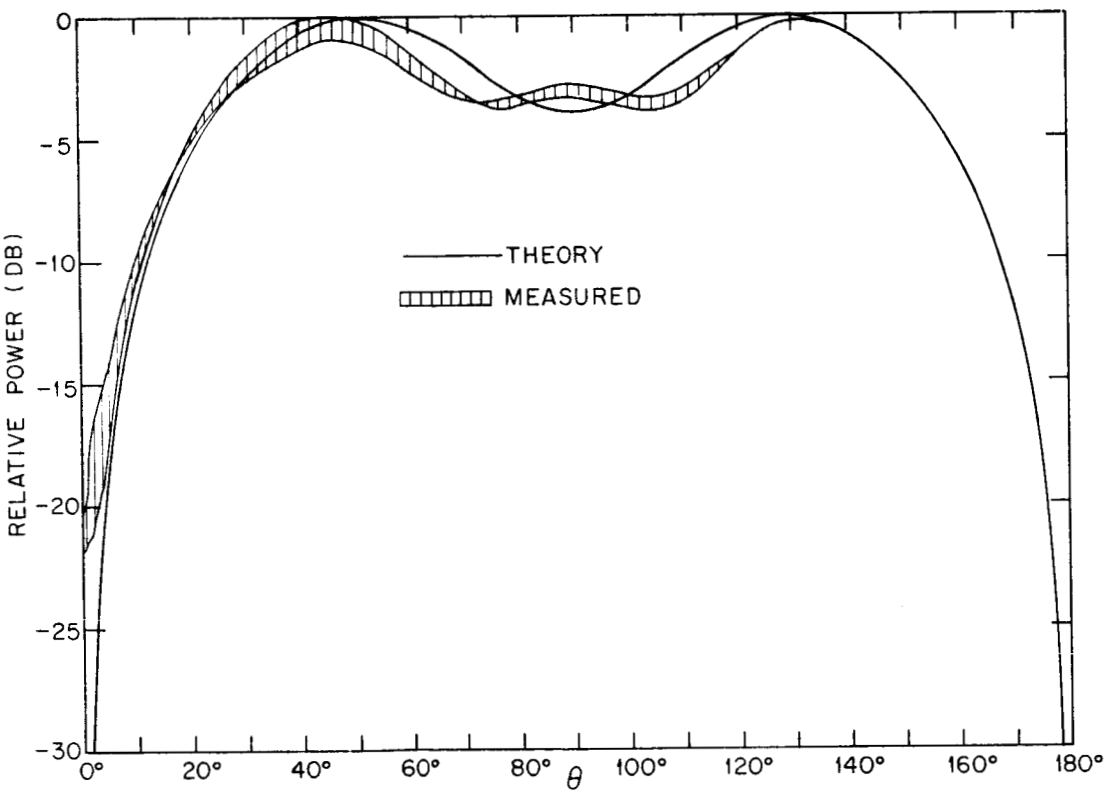

FIG. 26 FIELD PATTERN OF RESISTIVE DIPOLE ANTENNA AT 800 MHz

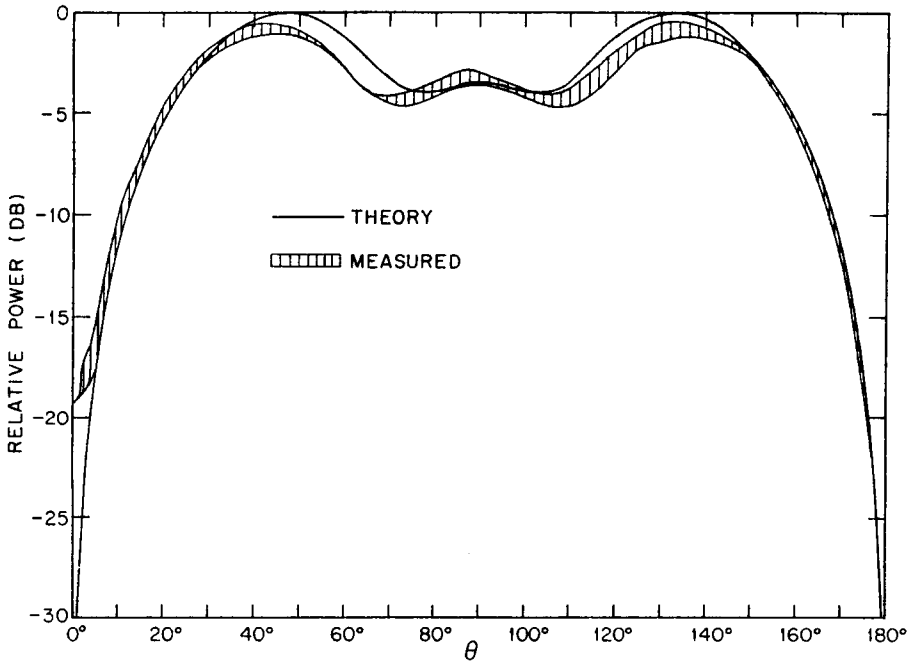

FIG. 27 FIELD PATTERN OF RESISTIVE DIPOLE ANTENNA AT f = 900 MHz

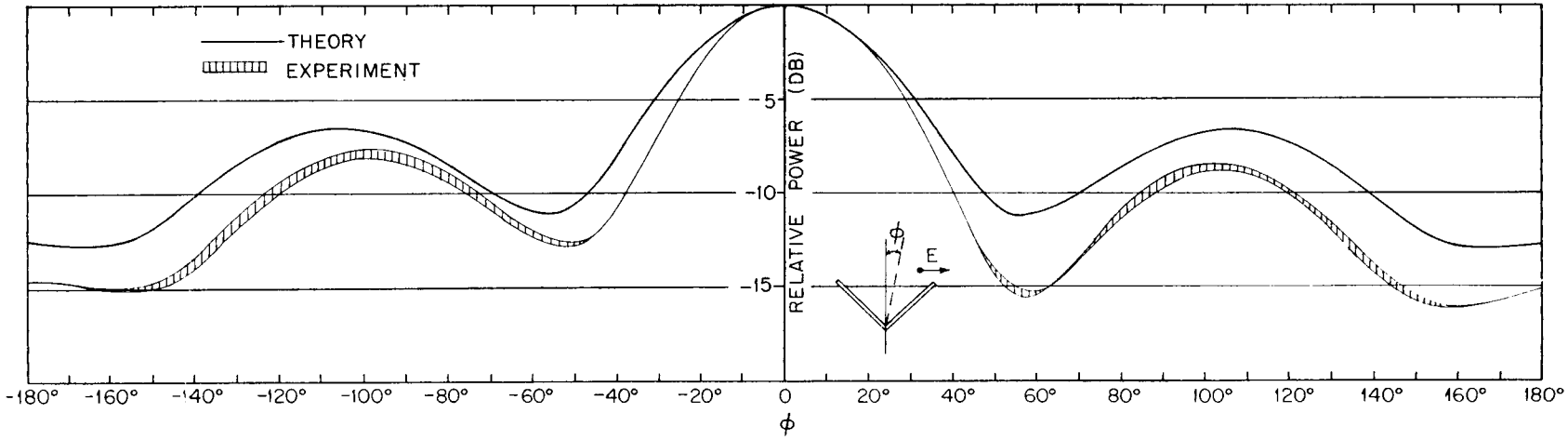

FIG. 28 FIELD PATTERN OF RESISTIVE 90°-V-ANTENNA AT 490 MHz

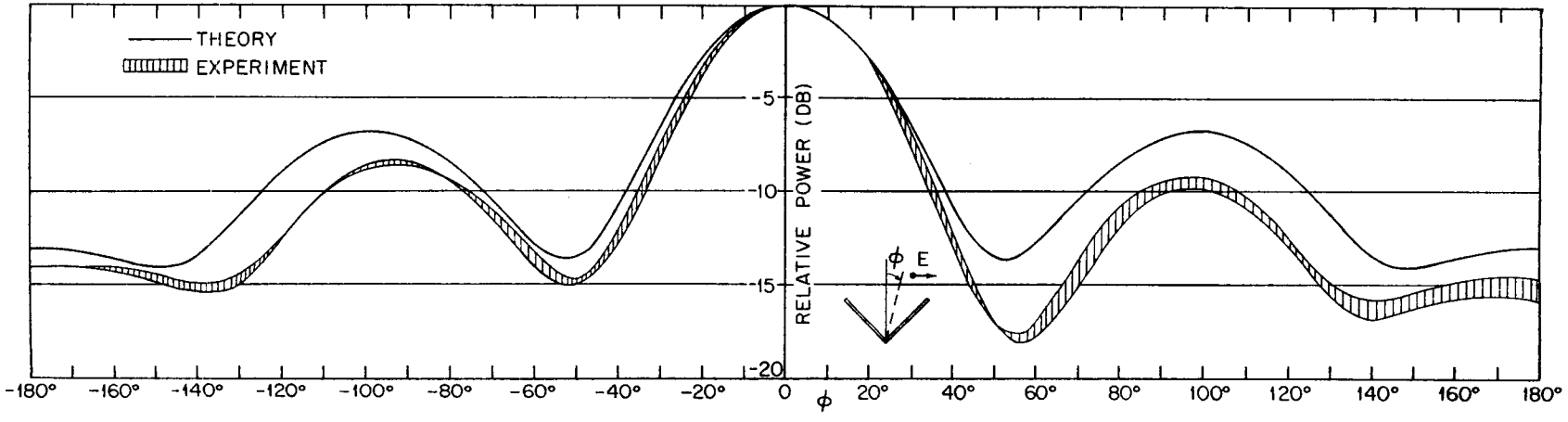

FIG. 29 FIELD PATTERN OF RESISTIVE 90°-V-ANTENNA AT 605 MHz

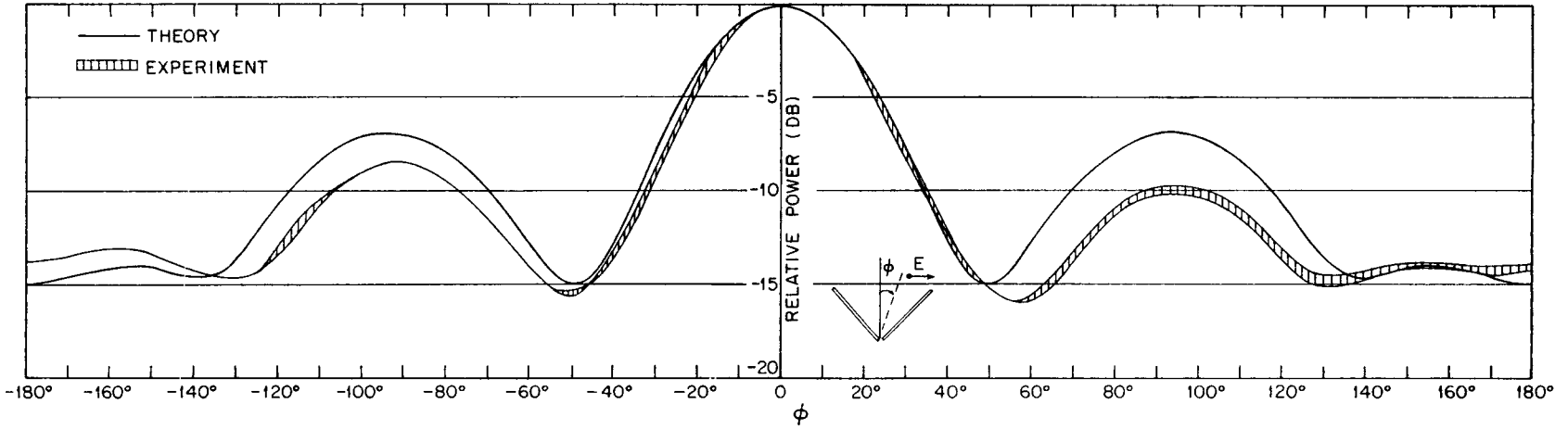

FIG. 30 FIELD PATTERN OF RESISTIVE 90°-V-ANTENNA AT 705 MHz

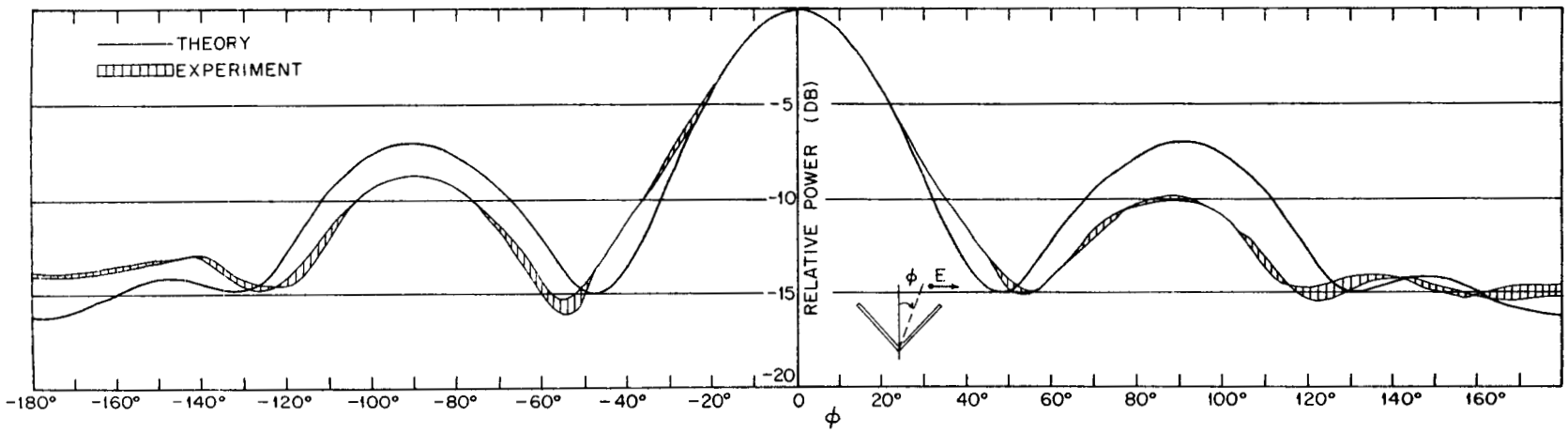

FIG. 31 FIELD PATTERN OF RESISTIVE 90°-V-ANTENNA AT 800 MHz

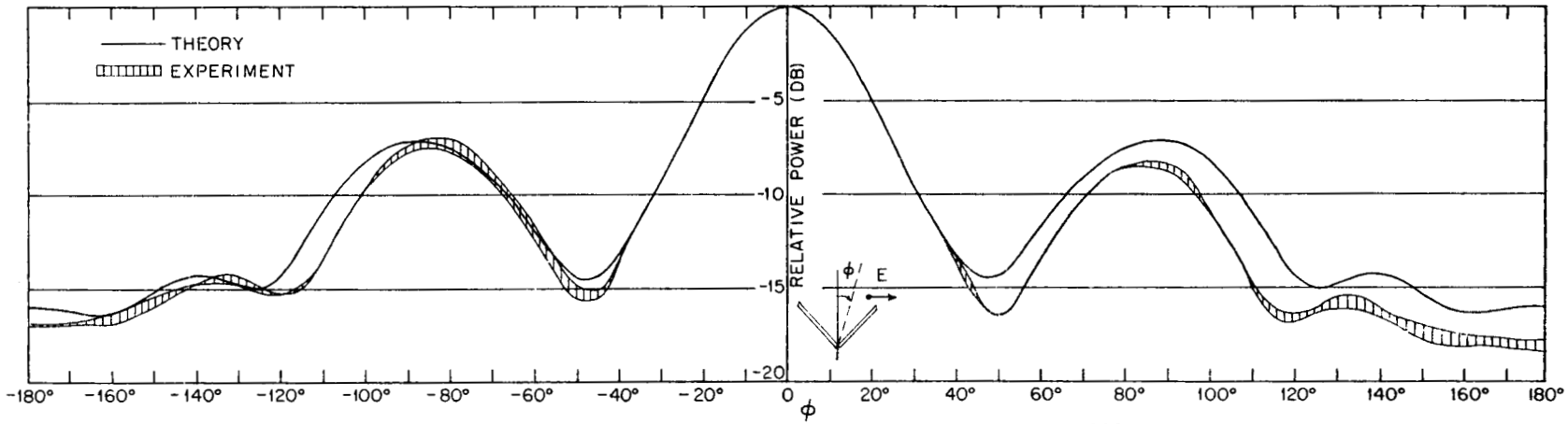

FIG. 32 FIELD PATTERN OF RESISTIVE 90°-V-ANTENNA AT 900 MHz

490 to 900 MHz. The change in width is considered to be small as compared with frequency change.

8. Conclusions

Antennas with step function z^i have been built to simulate the antenna with nonreflecting continuous resistive loading. In view of the analysis carried out in the previous report [3], the comparison between them is meaningful as long as the deviation of α from 1, which takes into account the discontinuity of z^i, is not large. The measured amplitude of the current distributions are found to decay linearly on the antenna, which agrees with the theory. The radiation field patterns have been measured and the agreement with the theory is in general good. The current, the input admittance, and the field pattern are found to be very insensitive to changes in frequency which is also anticipated successfully by the theory.

The zero-order theoretical input admittance does not agree well with the experimental data, but the theoretical input admittance of an infinitely long resistive antenna which is obtained by more rigorous Fourier Transform method with an approximated kernel, agrees with the experimental data remarkably well.

The radiation field pattern of a V-antenna with the angle between two arms of "V" equal to 90° has been measured when each arm of the antenna is made of a monopole antenna with nonreflecting step function z^i. The agreement between theory and experiment is again good. The front-to-back ratio of the V-antenna was found to be more than 14 db and the major lobes are at least 7 db higher than the minor lobes in the frequency

range of 490 to 900 MHz. The shape of the pattern is found to be very insensitive to changes in frequency.

The above evidence proves that the antenna with stepwise z^i does have a very broad frequency band and it seems that the existence of a traveling wave on its arms is suggested by the experimental results.

Although the antennas were built with a physical length equal to 50 cm only, the above conclusions seem to be rather general since the frequency range under which the antennas were tested is rather wide. It is believed that they should be applicable at least for antennas with electrical lengths not much greater than one wavelength.

It is observed from Fig. 16 that the imaginary part of the input admittance obtained from the zero-order theory does not agree with the experiment. It is seen that z^i on the dipole antenna with nonreflecting resistive loading is relatively constant near the driving point and the essential characteristic of this antenna is, just like an infinitely long resistive antenna, the existence of a traveling wave on its arms. Therefore it seems reasonable to suspect that its input admittance is close to that of an infinitely long resistive antenna which can be obtained by a more rigorous Fourier Transform method using an approximate kernel. The input conductance of an infinite antenna formed by a cylindrical tubular conductor of constant z^i has been studied by Shen and Wu [12]. The input susceptance of this antenna is obtained in the Appendix. It turns out that the theoretical value of the input admittance of an infinitely long tubular antenna of constant z^i is very close to that of the dipole antenna with nonreflecting resistive loading obtained experimentally (see Fig. 16a) .

While the input admittance of the infinite antenna is not sensitive to the value of z^i, as it can be seen in Fig. 2 of [12] and in Fig. 16a of this report, nevertheless physically this antenna and the dipole antenna with nonreflecting resistive loading do have a similar character and the agreement between the two sets of data of input admittance is thought to be more than a mere coincidence.

ACKNOWLEDGMENT

This subject was introduced to me by Professor Ronold W. P. King two years ago and without his patient guidance and many helpful suggestions which he has given me since then, this work could never have been completed. I am deeply grateful to him.

I wish to express my appreciation to Mr. E. J. Johnson who constructed the experimental apparatus.

REFERENCES

1. Altshuler, E. E., "The Traveling-Wave Linear Antenna," IRE Trans. AP-9, 324-329, July 1961; doctoral dissertation, Harvard University, May 1960.

2. Wu, T. T., and R. W. P. King, "The Cylindrical Antenna with Nonreflecting Resistive Loading," IEEE Trans. AP-13, No. 3, 369-373, May 1965; Scientific Report No. 1, Gordon McKay Lab., Harvard University, 1964.

3. Shen, L. C., and Wu, T. T., "The Cylindrical Antenna with Tapered Resistive Loading," Scientific Report No. 5, Gordon McKay Lab., Harvard University, August 1965.

4. Hatch, R. M. Jr., "Current Distribution on Conducting Sheets Excited by Arrays of Slot Antennas," Technical Report No. 103, Cruft Lab., Harvard University, July 1950.

5. Whiteside, H., "Electromagnetic Field Probes," Technical Report No. 377, Cruft Lab., Harvard University, October 1962.

6. King, R. W. P., Aronson, E. A. and Harrison, C. W. Jr., "Determination of the Admittance and Effective Length of Cylindrical Antennas," Radio Science, Vol. 1 (New Series), No. 7, 835-850, July 1966.

7. Morita, T., "The Measurement of Current and Charge Distributions on Cylindrical Antennas," Technical Report No. 66, Cruft Lab., Harvard University, February 1949.

8. King, R. W. P., "Fundamental Electromagnetic Theory," Dover, 1963.

9. Iizuka, K., "Experimental Studies of the Traveling-Wave V-Antenna and Related Antennas, Scientific Report No. 2, Gordon McKay Lab., Harvard University, October 1964.

10. Duff, B. M., "The Resistively Loaded V-Antenna," Scientific Report No. 3, Gordon McKay Lab., Harvard University, October 1964.

11. Iizuka, K., and King, R. W. P., "The Traveling-Wave V-Antenna," Scientific Report No. 4, Gordon McKay Lab., Harvard University, March 1965.

12. Shen, L. C., and Wu, T. T., "Radiated Power and Ohmic Loss of the Infinitely Long Cylindrical Antenna," Scientific Report No. 6, Gordon McKay Lab., Harvard University, February 1966.

13. Wu, T. T., "Theory of the Dipole Antenna and the Two-Wire Transmission Line," J. Math. Phys., Vol. II, No. 4, 550-574, July-August, 1961.

APPENDIX

In this appendix the input susceptance of the infinitely long tubular antenna of radius a, with uniform z^i, and driven by a delta-function generator, is evaluated. The Fourier Transform of the current I(z) on the antenna has been obtained in ref. 12, Eq. (2):

$$\bar{I}(\zeta) = \frac{4\pi i k}{\zeta_o} \quad \frac{1}{(k^2-\zeta^2)\,\bar{K}(\zeta) + \frac{4\pi i k z^i}{\zeta_o}} \tag{A-1}$$

The input susceptance of this antenna cannot be obtained by integration along the real axis of the imaginary part of the left-hand side of (A-1) since such an integration does not exist. The singularity of the imaginary part of the driving point current has been known to be a consequence of the assumption of the delta-function generator. In view of the success of the employment of an approximate kernel used as a substitute for the exact kernel $\bar{K}(\zeta)$ in Wu's theory on long antennas of infinite conductivity [13], in the sense that such a substitution yields a finite value of input admittance which agrees with the experimental result, the input admittance Y of this infinitely long resistive antenna is hereby defined as

$$Y = \frac{2ik}{\zeta_o} \int_{C_B} \frac{d\zeta}{(k^2-\zeta^2)\,[\Omega - 2\gamma + i\pi - \log(1-\zeta^2/k^2)] + ik^2 Z_R}, \quad Z_I = 0, \; Z_R < 2\pi \tag{A-2}$$

where C_B is the path wrapping the left branch cut shown in Fig. A-1.

This is permissible since for $Z_I = 0$, $Z_R < 2\pi$, the zeros near the branch points are in the next sheet of the Riemann surface. This is

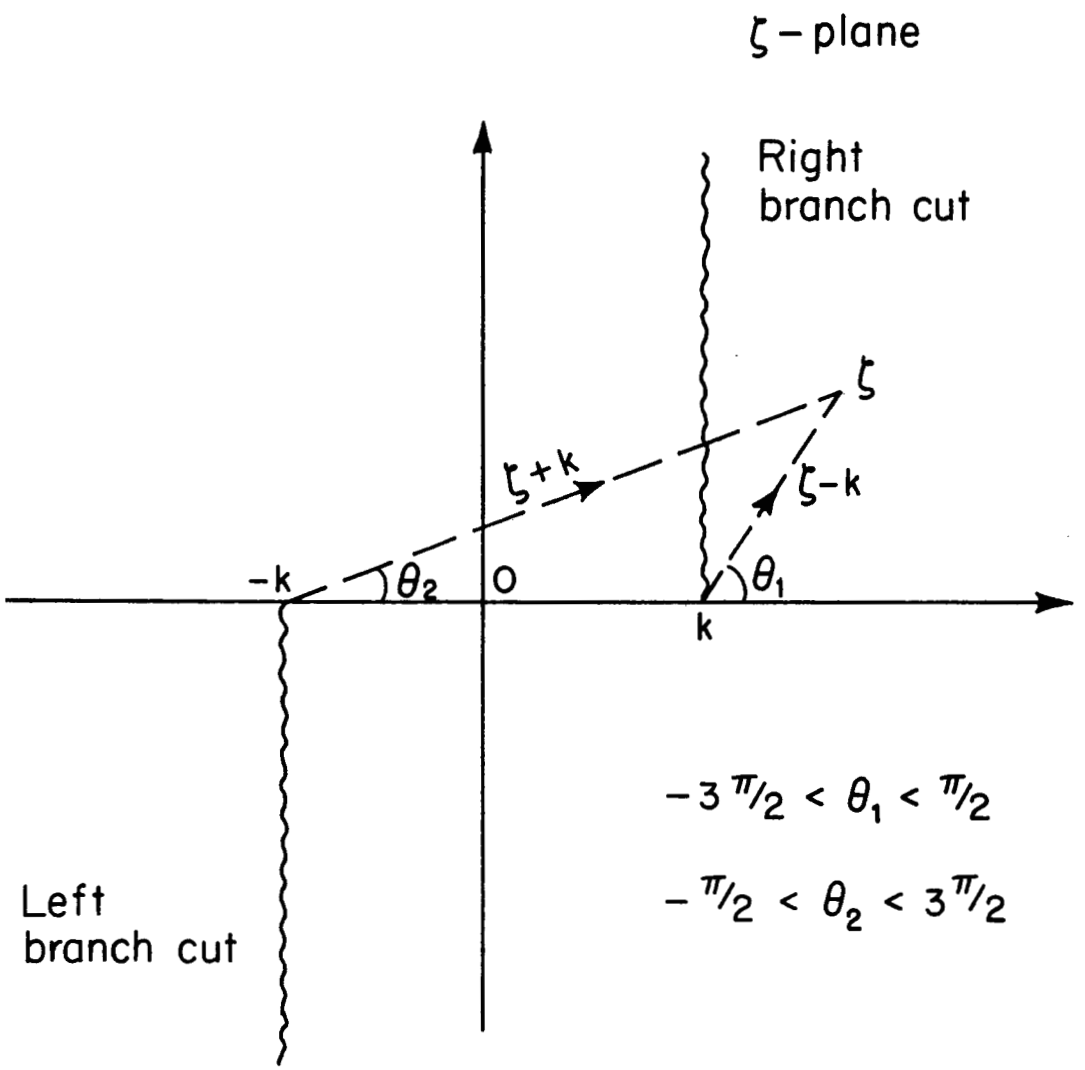

FIG. A-1 THE BRANCH CUTS OF $\overline{K}(\zeta)$

proved as follows.

The zero is near $\zeta=k$, thus the denominator of the integrand of (A-2) can be approximated and equated to zero as follows

$$(k^2-\zeta^2)\,[C-\log r_1 r_2 - i\,(\theta_1+\theta_2)] + ik^2 Z_R + k^2 Z_I = 0 \qquad \text{(A-3)}$$

where

$$kr_1 = |\zeta-k|,\quad kr_2 = |\zeta+k|,\quad -3\pi/2 \leq \theta_1 = \arg(\zeta-k) < \pi/2$$

and

$$-\pi/2 \leq \theta_2 = \arg(\zeta+k) < 3\pi/2\ .$$

Let

$\zeta=ky=k(1+utiv)$, (A-3) becomes

$$(v^2-2u-u^2)\,Q-2v(1+u)\,\theta+Z_I = 0 \qquad \text{(A-4)}$$

$$(v^2-2u-u^2)\,\theta+2v(1+u)\,Q-Z_R = 0 \qquad \text{(A-5)}$$

where

$$Q = C-\tfrac{1}{2}\ \log\,[(2+u)^2 + v^2]\,[u^2 + v^2]$$

and

$$\theta = \theta_1+\theta_2$$

Therefore

$$v \simeq Z_R/2Q \qquad \text{(A-6)}$$

and

$$u \simeq [Z_I + Z_R\,(Z_R-4\theta)/4Q]/2Q \qquad \text{(A-7)}$$

For $Z_R = Z_I$, the zero is at $\zeta_o = k\,[1+(Z_I+iZ_R)/2Q]$.

For $Z_I = 0$, $Z_R < 2\pi$, assume that u is positive, then $\theta \simeq -3\pi/2$, but (A-7) gives a negative u. If u is assumed to be negative, $\theta \simeq -3\pi/2$, but (A-7) gives a positive u. Therefore the zero is actually on the other Riemann surface, not on this defined in Fig. A-1. This completes the proof.

By a change of variable, (A-2) becomes

$$Y = \frac{2\pi}{\zeta_o} \int_o^\infty \frac{\eta(1+i\eta)\, d\eta}{\{\eta(1+i\eta)[C' - \frac{1}{2}\log \eta^2(1+\eta^2) - i(\frac{\pi}{2}+\theta)] - Z_R/4\}}$$

$$\{\eta(1+i\eta)\,[C' - \tfrac{1}{2}\log \eta^2(1+\eta^2) + i\,(\tfrac{3}{2}\,\pi - \theta)] - Z_R/4\}$$

for

$$Z_I = 0\,,\quad Z_R < 2\pi \qquad \text{(A-8)}$$

where

$$C' = \Omega - 2\gamma - 2\log 2$$

$$0 \leq \theta = \tan^{-1}\eta \leq \frac{\pi}{2}$$

Numerical integration of (A-8) shows that the real part of Y is equal to the input conductance obtained from previous calculations carried in [12], as it should be. The numerical value of the input admittance defined in this way has been calculated for an infinite antenna of radius $a = 0.3175$ cm and z^i ranging from 720 to 1440 ohms per meter at frequency ranging from 450 to 900 MHz. The result is shown in Fig. 16a.

Unclassified

Security Classification

DOCUMENT CONTROL DATA - R&D

(Security classification of title, body of abstract and indexing annotation must be entered when the overall report is classified)

1. ORIGINATING ACTIVITY *(Corporate author)*
Division of Engineering and Applied Physics
Harvard University, Cambridge, Mass.

2a. REPORT SECURITY CLASSIFICATION
Unclassified

2b. GROUP

3. REPORT TITLE

AN EXPERIMENTAL STUDY OF THE DIPOLE ANTENNA WITH NONREFLECTING RESISTIVE LOADING

4. DESCRIPTIVE NOTES *(Type of report and inclusive dates)*
Scientific report

5. AUTHOR(S) *(Last name, first name, initial)*

Shen, Liang-Chi

6. REPORT DATE	7a. TOTAL NO. OF PAGES	7b. NO. OF REFS
September, 1966	62	13

8a. CONTRACT OR GRANT NO.	9a. ORIGINATOR'S REPORT NUMBER(S)
NsG-579	Scientific Report No. 7
b. PROJECT NO.	
c.	9b. OTHER REPORT NO(S) *(Any other numbers that may be assigned this report)*
d.	

10. AVAILABILITY/LIMITATION NOTICES

Reproduction in whole or in part is permitted by the U. S. Government. Distribution of this document is unlimited.

11. SUPPLEMENTARY NOTES	12. SPONSORING MILITARY ACTIVITY

13. ABSTRACT

The amplitude of the current, the input admittance, and the radiation field pattern of a cylindrical antenna with a step-function internal impedance are measured in the frequency range 450 to 900 MHz. Several designs of the step-function are tried in order to simulate the antenna with the smoothly distributed resistive loading which has been studied in previous reports. The experimental result is compared with the theory. It is pointed out that such comparison is meaningful in the light of the analysis carried out in previous reports. It has been found that the zero-order theory gives accurate descriptions of the current distribution, the field pattern, the property of a very broad frequency band of the antenna, and the existence of the traveling wave on the antenna. The agreement of the input admittance is not good, but it is found that the theoretical input admittance of the infinitely long resistive antenna which is obtained by a Fourier Transform method fits the experimental data satisfactorily.

DD FORM 1 JAN 64 1473

Unclassified

Security Classification

14. KEY WORDS	LINK A		LINK B		LINK C	
	ROLE	WT	ROLE	WT	ROLE	WT
experiment dipole antenna with nonreflecting resistive loading traveling wave directional wide frequency band current distribution input admittance field pattern						

INSTRUCTIONS

1. ORIGINATING ACTIVITY: Enter the name and address of the contractor, subcontractor, grantee, Department of Defense activity or other organization *(corporate author)* issuing the report.

2a. REPORT SECURITY CLASSIFICATION: Enter the overall security classification of the report. Indicate whether "Restricted Data" is included. Marking is to be in accordance with appropriate security regulations.

2b. GROUP: Automatic downgrading is specified in DoD Directive 5200.10 and Armed Forces Industrial Manual. Enter the group number. Also, when applicable, show that optional markings have been used for Group 3 and Group 4 as authorized.

3. REPORT TITLE: Enter the complete report title in all capital letters. Titles in all cases should be unclassified. If a meaningful title cannot be selected without classification, show title classification in all capitals in parenthesis immediately following the title.

4. DESCRIPTIVE NOTES: If appropriate, enter the type of report, e.g., interim, progress, summary, annual, or final. Give the inclusive dates when a specific reporting period is covered.

5. AUTHOR(S): Enter the name(s) of author(s) as shown on or in the report. Enter last name, first name, middle initial. If military, show rank and branch of service. The name of the principal author is an absolute minimum requirement.

6. REPORT DATE: Enter the date of the report as day, month, year; or month, year. If more than one date appears on the report, use date of publication.

7a. TOTAL NUMBER OF PAGES: The total page count should follow normal pagination procedures, i.e., enter the number of pages containing information.

7b. NUMBER OF REFERENCES: Enter the total number of references cited in the report.

8a. CONTRACT OR GRANT NUMBER: If appropriate, enter the applicable number of the contract or grant under which the report was written.

8b, 8c, & 8d. PROJECT NUMBER: Enter the appropriate military department identification, such as project number, subproject number, system numbers, task number, etc.

9a. ORIGINATOR'S REPORT NUMBER(S): Enter the official report number by which the document will be identified and controlled by the originating activity. This number must be unique to this report.

9b. OTHER REPORT NUMBER(S): If the report has been assigned any other report numbers *(either by the originator or by the sponsor)*, also enter this number(s).

10. AVAILABILITY/LIMITATION NOTICES: Enter any limitations on further dissemination of the report, other than those imposed by security classification, using standard statements such as:

(1) "Qualified requesters may obtain copies of this report from DDC."

(2) "Foreign announcement and dissemination of this report by DDC is not authorized."

(3) "U. S. Government agencies may obtain copies of this report directly from DDC. Other qualified DDC users shall request through _____."

(4) "U. S. military agencies may obtain copies of this report directly from DDC. Other qualified users shall request through _____."

(5) "All distribution of this report is controlled. Qualified DDC users shall request through _____."

If the report has been furnished to the Office of Technical Services, Department of Commerce, for sale to the public, indicate this fact and enter the price, if known.

11. SUPPLEMENTARY NOTES: Use for additional explanatory notes.

12. SPONSORING MILITARY ACTIVITY: Enter the name of the departmental project office or laboratory sponsoring *(paying for)* the research and development. Include address.

13. ABSTRACT: Enter an abstract giving a brief and factual summary of the document indicative of the report, even though it may also appear elsewhere in the body of the technical report. If additional space is required, a continuation sheet shall be attached.

It is highly desirable that the abstract of classified reports be unclassified. Each paragraph of the abstract shall end with an indication of the military security classification of the information in the paragraph, represented as *(TS), (S), (C), or (U)*.

There is no limitation on the length of the abstract. However, the suggested length is from 150 to 225 words.

14. KEY WORDS: Key words are technically meaningful terms or short phrases that characterize a report and may be used as index entries for cataloging the report. Key words must be selected so that no security classification is required. Identifiers, such as equipment model designation, trade name, military project code name, geographic location, may be used as key words but will be followed by an indication of technical context. The assignment of links, roles, and weights is optional.